Nfkbid is required for immunity and antibody responses to *Toxoplasma gondii*

Scott P. Souza[1,3], Samantha D. Splitt[1,3], Julia A. Alvarez[1,3], Juan C. Sanchez-Arcila[1], Jessica N. Wilson[1,3], Safuwra Wizzard[1], Zheng Luo[4], Nicole Baumgarth[4], Kirk D.C. Jensen[1, 2#]

[1]School of Natural Sciences, Department of Molecular and Cell Biology, University of California, Merced

[2]Health Science Research Institute, University of California, Merced

[3]Graduate Program in Quantitative and Systems Biology, University of California, Merced

[4]Center for Immunology & Infectious Diseases, and Department of Pathology, Microbiology and Immunology, University of California, Davis

[#]**Email:** kjensen5@ucmerced.edu

Keywords: B-1 cells, B-2 cells, isotype class switching, *Nfkbid*, IkBNS, *Toxoplasma gondii*, atypical strains, recombinant inbred mice, QTL, vaccines

SUMMARY (150 word limit)

Protective immunity to parasitic infections has been difficult to elicit by vaccines. Among parasites that evade vaccine-induced immunity is *Toxoplasma gondii*, which causes lethal secondary infections in chronically infected mice. To identify correlates of immunity, mouse genetics were used to identify *Nfkbid*, a nuclear regulator of NF-κB that is required for B cell activation and B-1 cell development. *Nfkbid*-null mice (bumble) did not generate parasite-specific IgM and lacked robust parasite-specific IgG, which correlated with defects in B-2 cell maturation and class-switch recombination. Though high-affinity antibodies were B-2 derived, transfer of B-1 cells partially rescued the immunity defects observed in bumble and bone marrow chimeric mice. Immunity in resistant mice correlated with robust isotype class-switching in both B cell lineages, which can be fine-tuned by *Nfkbid* gene expression. We propose a model whereby humoral immunity to *T. gondii* is regulated by *Nfkbid* and requires B-1 and B-2 cells for full protection.

INTRODUCTION

The goal of vaccination is to induce immunological memory that can protect from natural infection challenge. Depending on the pathogen, effective memory would need to protect also against a wide variety of pathogen-specific strains encountered in nature. Such protection is termed heterologous immunity and is effective against pathogen strains that differ in virulence, immune evasion, or polymorphic antigens. Parasites represent a special challenge to vaccine development. Indeed, an entirely protective vaccine has yet to be achieved for any human parasite (Sacks, 2014). The apicomplexan parasite *Toxoplasmas gondii*, provides an excellent system to explore requirements for heterologous immunity to a parasitic pathogen. *T. gondii* is a globally spread intracellular protozoan parasite of warm-blooded animals that exhibits great genetic diversity (Lorenzi et al., 2016). *T. gondii*

49 strains differ dramatically in primary infection virulence in laboratory mice (Howe and
50 Sibley, 1995) and in severity of human toxoplasmosis (Grigg et al., 2001; Khan et al.,
51 2006; McLeod et al., 2012). Such infections can be overcome by immunological memory
52 responses elicited by vaccination or natural infection. In particular, memory CD8 T cells
53 and induction of IFNγ are primarily responsible for protection against lethal secondary
54 infections with the widely studied type I RH strain, which has a lethal dose of one parasite
55 in naïve mice (Gazzinelli et al., 1991; Gigley et al., 2009; Suzuki, Y. and Remington, 1990).
56 CD4 T cells are required to help the formation of effector CD8 T cell (Casciotti et al., 2002)
57 and B cell responses (Johnson and Sayles, 2002), but the ability to adoptively transfer
58 vaccine-elicited cellular immunity to naïve recipients against the type I RH challenge is
59 unique to memory CD8 T cells (Gazzinelli et al., 1991; Gigley et al., 2009).

60 The role of B cells in *T. gondii* infections is less understood. Previous studies
61 showed that B cell deficient mice (muMT) are extremely susceptible to primary (Chen et
62 al., 2003), chronic (Kang et al., 2000) and secondary infections (Sayles et al., 2000),
63 despite unimpaired levels of IFNγ. Passive transfer of antibodies from immunized animals
64 into vaccinated muMT mice significantly prolongs their survival after challenge (Johnson
65 and Sayles, 2002; Sayles et al., 2000). IgM seems particularly suited for blocking cellular
66 invasion by *T. gondii* (Couper et al., 2005), while IgG can perform both neutralization
67 (Mineo et al., 1993) and opsonization functions (Joiner et al., 1990). Antibody responses
68 against *T. gondii* are dependent on CD4 T cells (Glatman Zaretsky et al., 2012; Johnson
69 and Sayles, 2002), and are regulated by cytokines that modulate T follicular helper cell
70 and germinal center B cell formation in secondary lymphoid organs (Stumhofer et al.,
71 2013), suggesting conventional “B-2” B cell responses provide antibody-mediated
72 immunity to *T. gondii.*

73 In addition, “B-1” cells are innate-like lymphocytes that are known for producing
74 self- and pathogen-reactive “natural” IgM. B-1 cells are the predominant B cell
75 compartment within the body cavities, including the peritoneal and pleural spaces and
76 contribute to antigen-specific responses to many pathogens. In mouse models of
77 secondary bacterial infections, including *Borrelia hermsii*, *Streptococcus pneumoniae* and
78 non-typhoid *Salmonella,* vaccination induces protective memory B-1 cells to T cell-
79 independent bacterial antigens (reviewed in (Smith and Baumgarth, 2019)). This memory
80 is often restricted to the B-1(b), or CD5- subset of B-1 cells (Alugupalli et al., 2004), but
81 not in all models (Yang et al., 2012). In the *T. gondii* model, one study suggested that
82 primed CD5+ B-1(a) cells can rescue B-cell-deficient mice during primary infection with a
83 low virulence strain (Chen et al., 2003). Memory B cells are also appreciated to secrete
84 pathogen-specific IgM (Pape et al., 2011), and generate somatically mutated IgM to
85 combat blood stage secondary infection with *Plasmodium* (Krishnamurty et al., 2016).
86 Whether IgM responses to *T. gondii* are B-2 or B-1 derived is unknown. Moreover, the role
87 of B-1 cells in promoting immunity to *T. gondii* during a secondary infection has yet to be
88 determined.

89 Particularly troubling for vaccine development for *T. gondii* is the lack of sterilizing
90 immunity achieved following infection (Jensen et al., 2015). Unlike the highly passaged
91 lab type I RH strain, for which most immunological memory studies have been performed,
92 the less passaged type I GT1 strain and atypical strains, many of which are endemic to
93 South America, cause lethal secondary infections in C57BL/6J mice and co-infect (i.e.
94 “superinfect”) the brains of challenged survivors (Jensen et al., 2015). During secondary
95 infection memory CD8 T cells become exhausted, but checkpoint blockade fails to reverse
96 disease outcome (Splitt et al., 2018). The data suggest yet unknown mechanisms are
97 needed to provide heterologous immunity to highly virulent strains of *T. gondii*. Therefore,

98 we set out to address whether additional requirements are necessary for heterologous
99 immunity to *T. gondii*. Through use of forward and reverse genetics, we discovered a
100 previously unidentified essential role for *Nfkbid* in immunity and antibody responses to *T.*
101 *gondii*, and present evidence that both B-1 and B-2 cells assist resistance to secondary
102 infection with highly virulent parasite strains.
103

104 **RESULTS**

105 **Non-MHC loci control resistance to secondary infection with *Toxoplasma gondii***

106 When mice are given a natural infection with a low virulent type III CEP strain and
107 allowed to progress to chronic infection for 35-42 days, the immunological memory that
108 develops is known to protect against secondary infections with the commonly studied lab
109 strain, type I RH. In contrast, highly virulent "atypical" strains such as those isolated from
110 South America (VAND, GUYDOS, GUYMAT, TgCATBr5) or France (MAS, GPHT, FOU)
111 and the clonal type I GT1 strain led to morbidity and mortality in C57BL/6J mice at varying
112 frequencies, depending on the strain type and their virulence factors (Jensen et al., 2015).
113 To explore whether host genetics influenced the ability to survive secondary infection, a
114 similar experiment was performed with A/J mice. In contrast to C57BL/6 mice, A/J mice
115 were resistant to secondary infection with all virulent atypical *T. gondii* strains analyzed
116 (Fig 1A) and cleared parasite burden as early as day 4 post challenge (Fig 1B). In contrast,
117 naïve A/J mice succumb to infections with atypical strains (not shown). These results
118 suggest that at least one or more genetic loci controls immunity to virulent challenge.

119 A/J mice are known to be resistant to primary infections with the intermediate
120 virulent type II strain (McLeod et al., 1989), and prevent cyst formation due to
121 polymorphisms in their MHC class I H-2 molecule, L^d (Brown et al., 1995). To test whether
122 the H-2 locus contributes to immunity we compared secondary infections in C57BL/10

123 (B10) and C57BL/10.A (B10.A) mouse strains, the latter carrying the MHC H-2 locus of
124 A/J (H-2a) in place of C57BL/6's MHC H-2 (H-2b). Compared to mice with the H-2b
125 haplotype, mice expressing H-2a had less cysts and weighed more during chronic
126 infection with type III strains ($P<0.04$; Fig S1). Despite their relative health at the time of
127 challenge, B10.A mice were highly susceptible (0%-30% survival) to secondary infection
128 with certain atypical strains (VAND, GUY-DOS, GPHT, FOU), but displayed varying
129 degrees of resistance to others (TgCATBr5, MAS, GUY-MAT; 60-100% survival) (Fig 1A).
130 In the case of MAS secondary infection, B10.A mice but not B10 mice were highly resistant
131 and exhibited reduced parasite burden by day 8 post challenge (Fig 1B). Together, the
132 data suggest that while the MHC H-2a locus is an important modifier of resistance to
133 certain *T. gondii* strains, this is not true for every challenge. Importantly, the A/J genetic
134 background encodes additional non-MHC-linked genes that control immunity to *T. gondii*.

135 **Genetic mapping reveals four loci that correlate with immunity to *Toxoplasma***
136 ***gondii***

137 To identify non-MHC loci that promote resistance to secondary infection, we first
138 analyzed the outcome of infection with the type I GT1 *T. gondii* strain, as this strain caused
139 lethal secondary infections in B10 and B10.A, but not in A/J or first filial generation A/J x
140 C57BL/6J mice ('F1') (Fig 1C). Following secondary infections, A/J and F1 mice showed
141 no overt symptoms of weight loss, dehydration, or lethargy (not shown). However, sterile
142 immunity was not achieved. For example, the GT1 strain was present in the brains of
143 these survivors (i.e. "superinfection"), and at greater frequencies in F1 compared to A/J
144 mice (Fig 1D). Superinfections were also detected at high frequencies in B10 and B10.A
145 surviving mice challenged with atypical strains. Overall, mice of the C57BL genetic
146 background were more prone to superinfection compared to A/J mice (Table S1). It is
147 unknown whether virulent strains of *T. gondii* have evolved to superinfect hosts with

148 immunological memory, as previously hypothesized(Jensen et al., 2015). Nonetheless,
149 our results underscore the difficulty in achieving sterile immunity to parasites in otherwise
150 genetically resistant hosts.

151 Then we performed secondary infection experiments with the type I GT1 strain
152 using 26 recombinant inbred (RI) mice (Table S2). The AxB:BxA RI mouse panel contains
153 an assortment of homozygous A/J and C57BL/6 alleles, which assist genetic mapping of
154 loci that contribute to various phenotypes, including those related to *T. gondii* infection
155 (Hassan et al., 2015; McLeod et al., 1989). Genetic mapping revealed four distinct
156 Quantitative Trait Loci (QTL) peaks with logarithm of the odds (LOD) scores greater than
157 3 on chromosomes 7, 10, 11 and 17 (Fig 2A). None of the QTLs bore evidence for epistatic
158 interactions (not shown), and only the chromosome 10 QTL surpassed genome-wide
159 permutation testing (n=1000, $P<0.05$). Nevertheless, an additive-QTL model including all
160 four QTLs best fit the data compared to any lesser combination of them ($P<0.02$, ANOVA).
161 The estimated effect on the phenotypic variance observed in the RI panel is 24%, 41%,
162 21% and 27% for the chromosome (chr) 7, 10, 11 and 17 QTLs, respectively. Consistent
163 with these estimates, complete phenotypic penetrance (i.e. allelic correlation at 100%)
164 was not observed for any locus (Fig 2B). Moreover, replacing chromosomes 7 or 10 of
165 C57BL/6J with those of A/J conferred no survival advantage to secondary infection in
166 consomic mice (Fig S2). Regardless, small effect QTLs controlling complex traits can still
167 lead to the identification of causal genes within a QTL region, as occurred for the
168 successful identification of MHC 1 L^d as the host resistance factor to chronic *T. gondii*
169 infection (Brown et al., 1995).

170 *Nfkbid* is one of the most polymorphic genes within the chr7 QTL region (Mb 30.3-
171 33.0) and sits between the genetic markers that flank the highest imputed LOD score
172 (Dataset S1). This gene encodes IκBNS, which is a member of atypical NF-κB inhibitors,

173 called nuclear IκBs, reflecting their restricted cellular localization. Unlike classical inhibitors
174 of NF-κB, atypical NF-κB inhibitors can modulate NF-κB to induce or repress transcription
175 (Schuster et al., 2013). Previous work has shown that *Nfkbid* null mice completely fail to
176 develop B-1 cells, lack circulating IgM and IgG3 antibodies, and cannot respond to T-
177 independent (T-I) type II antigens such as NP-ficoll (Arnold et al., 2012; Pedersen et al.,
178 2016; Touma et al., 2011). IκBNS also promotes early plasma blast differentiation
179 (Khoenkhoen et al., 2019) and IgG1 responses to model T-dependent antigens (Arnold et
180 al., 2012; Hosokawa et al., 2017; Touma et al., 2011), enhances T cell production of IL-2
181 and IFNγ (Touma et al., 2007), supports development of T regulatory cells (Schuster et
182 al., 2012) and suppresses TLR-induced cytokine expression in macrophages (Kuwata et
183 al., 2006). The tetraspanin, *Tspan8,* is within the chr10 QTL (Mb 115.8-116.2) and is the
184 most highly polymorphic gene between A/J and C57BL/6J mice in this region (Dataset
185 S1). *Tspan8* is 6-fold more highly expressed in spleens from A/J compared to C57BL/6
186 mice (immgen.org). *Tspan8* promotes cancer metastasis (Berthier-Vergnes et al., 2011)
187 and can impact leukocyte migration (Zhao et al., 2018), but its role in immunity is largely
188 unknown. Other polymorphic gene candidates within the four QTLs are listed in Dataset
189 S1.

190 ***Nfkbid* on chromosome 7 is required for immunity and the generation of**
191 ***Toxoplasma gondii*-specific antibodies**

192 Given the role of *Nfkbid* in several immune functions, degree of polymorphism and
193 central location within the chr7 QTL, the requirement for *Nfkbid* in immunity to *T. gondii*
194 was further explored. *Nfkbid* null "bumble" mice (C57BL/6) have previously been
195 described, which were derived from an ENU mutagenesis screen. These mice possess a
196 premature stop codon in *Nfkbid,* rendering them unable to support T-I antibody responses
197 and B-1 development (Arnold et al., 2012). Bumble mice survived primary infection with

198 the low virulent CEP strain at frequencies similar to wildtype C57BL/6J mice (Fig 2C) but
199 succumbed to secondary infection three days earlier when challenged with the GT1 strain
200 (Fig 2D). Since the C57BL genetic background is uniformly susceptible to GT1 secondary
201 infections used in our genetic screen, susceptibility to challenge with the commonly
202 studied type I RH strain was explored, which is normally controlled in vaccinated or
203 chronically infected mice (Gazzinelli et al., 1991; Gigley et al., 2009; Suzuki, Y. and
204 Remington, 1990). Importantly, bumble mice were entirely susceptible to secondary
205 infection with the type I RH strain (Fig 2E), which exhibited greater parasite loads
206 compared to wildtype mice (Fig 2F). Moreover, bumble mice failed to generate parasite
207 specific-IgM, and were poor producers of parasite-specific IgG3, IgG2b and IgG2a
208 antibody responses after chronic infection (Fig 3A). The remaining antibodies that were
209 secreted exhibited defects in their ability to block parasite invasion of host cells (Fig 3B).
210 Antibodies from naïve mice fail to bind *T. gondii*, thus natural antibodies do not recognize
211 *T. gondii,* consistent with previous reports (Couper et al., 2005). Although *Nfkbid* promotes
212 T cell production of IFNγ and IL-2 in in vitro stimulation assays (Touma et al., 2007) and
213 promotes thymic development of FOXP3+ T regulatory cells (Schuster et al., 2012), no
214 impairment of T cell cytokine production was observed, nor were frequencies of FOXP3+
215 $CD25^{hi}$ CD4+ T regulatory cells altered in bumble compared to wildtype mice during
216 secondary infection (Fig S3).

217 To determine where the breakdown in the B cell response occurred in bumble
218 mice, immunophenotyping was employed. Consistent with previous reports, bumble mice
219 have greatly reduced marginal zone B cells in naïve mice and did not increase in frequency
220 during *T. gondii* infection (not shown). Atypical B cells (FCLR5+ CD80+ CD73+) which
221 respond to *Plasmodium* infections in mice (Kim et al., 2019) were also reduced in bumble
222 compared to B6 mice following *T. gondii* infection (not shown). The memory CD73+ B cell

223 compartment in bumble mice bore evidence for reduced class switching during *T. gondii*
224 infection, as they remain mainly IgM+IgD+ while C57BL/6J mice have higher frequencies
225 of IgM-IgD- cells (Fig 3C). Most pronounced, however, is a large accumulation of
226 transitional stage immature B-2 cells in bumble mice that occurs during chronic infection,
227 implicating that B cell responses to *T. gondii* may require reinforcement from recent bone
228 marrow derived emigrants that is blocked in the absence of *Nfkbid*. Hence, *Nfkbid* is not
229 only an important regulator of B-1 cell development through the transitional stage of
230 immature B cell development in the steady state (Pedersen et al., 2014), but also for B-2
231 cell maturation, differentiation and activation during *T. gondii* infection.

232 **Defective B-1 and B-2 responses underlie bumble's defect in immunity**

233 The impaired ability of bumble mice to generate parasite-specific antibodies,
234 combined with the documented collapse of the B-1 cell compartment in *Nfkbid*-deficient
235 mice (Arnold et al., 2012; Touma et al., 2011), prompted us to directly assess the role of
236 B-1 mediated immunity and humoral responses to *T. gondii*. First, total peritoneal exudate
237 cells (PerC) were adoptively transferred into bumble mice at day 2 of birth, which allows
238 optimal B-1 engraftment and self-renew for the life of the animal (Baumgarth et al., 2000).
239 Then, bumble mice that received total PerC transfers were infected with the avirulent type
240 III strain at 6-7 weeks of age and given a secondary infection 35 days later with the type I
241 RH strain (Fig 4A). Bumble mice receiving PerC partially reconstituted serum IgM to ~40%
242 of wildtype levels (Fig S4A), consistent with previous studies (Baumgarth et al., 2000),
243 and had a significantly delayed time to death relative to non-transferred littermates
244 following type I RH challenge (Fig 4A). Previous studies have shown B-1 cells respond to
245 infections and create both pathogen- (Alugupalli et al., 2004; Choi and Baumgarth, 2008)
246 and microbiota -specific antibodies (Kreuk et al., 2019). Antibody profiling of bumble mice
247 that received PerC transfer showed a trend of increased anti-*T. gondii* antibody generation

248 following chronic infection (Fig 4B), but antibody reactivity to the parasite did not reach
249 levels observed in wildtype mice, suggesting the B-1 compartment has a limited role in
250 generating high-affinity parasite-specific antibodies. The B cell compartment responsible
251 for generating parasite-specific antibody was further confirmed with Igh-allotype chimeric
252 mice which allow tracking of IgM responses of allotype-marked B-1 and B-2 cells (Lalor et
253 al., 1989). In this experimental setup, endogenous B cells of the C57BL/6 background
254 (IgH-b allotype) are depleted with allotype specific anti-IgM-b antibodies and replaced with
255 transferred PerC B-1 of the IgH-a allotype which are refractory to the depletion antibodies
256 and will engraft for the life of the animal. Following removal of the depleting antibodies,
257 the endogenous B-2 cell population reemerge and are marked with anti-IgM-b antibodies,
258 while the transferred B-1 cell are marked with anti-IgM-a antibodies (Fig 4C). Assessing
259 antibody responses generated in IgH-allotype chimeric mice during a *T. gondii* infection
260 revealed the presence of B-1 derived IgM-a antibodies that had low reactivity to *T. gondii*
261 at days 14 and 30 post-infection, but the majority of highly reactive parasite-specific IgM-
262 b was derived from the B-2 compartment (Fig 4D).

263 Attempts to explore the role of B-1 and B-2 cells utilizing B cell deficient muMT
264 mice were complicated by their high susceptible to primary infection with the CEP strain,
265 irrespective of whether they received PerC as neonates or splenic B-2 cells prior to the
266 primary infection (Fig S4C-E), thus underscoring the importance of B cells in resistance to
267 *T. gondii* infection (Kang et al., 2000). Instead, mixed bone marrow chimeras were
268 generated in which irradiated bumble or wildtype recipients were transferred wildtype or
269 bumble bone marrow to reconstitute B-2 cells and the rest of the hematopoietic
270 compartment. Since B-1a cells do not efficiently reconstitute irradiated recipients from
271 adult bone marrow (Kantor et al., 1992), some recipients received wildtype PerC to restore
272 the B-1 compartment in this setting (Choi and Baumgarth, 2008). These and other bone

273 marrow chimeras (not shown) all succumbed to primary CEP infections (Fig S5). To
274 bypass the susceptibility of irradiated bone marrow recipients to live *T. gondii* infections
275 (Yap and Sher, 1999), bone marrow chimeras were vaccinated with a replication deficient
276 uracil auxotroph strain (RH *Δompdc Δup*) improving overall survival (Fig S5). Whereas
277 vaccinated wildtype recipient mice that received *Nfkbid*-sufficient but not bumble bone
278 marrow were able to survive type I RH challenge (Fig 4E), complete immunity was
279 conferred only when they were transferred PerC. This study also suggests that *Nfkbid* is
280 important in the non-hematopoietic lineage, as complete immunity was restored only in
281 wildtype but not bumble recipients (Fig 4E). In summary, our reconstitution studies
282 emphasize the importance of *Nfkbid* sufficiency in multiple compartments and highlight B-
283 1 cells as an important contributor to *T. gondii* immunity.

284 **Evidence for enhanced B-1 and B-2 cell activation in resistant A/J mice**

285 Since *Nfkbid* has a profound effect on the maturation and activation of multiple B
286 cell populations in the C57BL/6J background, we extended our analysis of the humoral
287 response to the resistant A/J background. A/J mice were found to have a superior IgG
288 response to parasite lysate antigen during secondary infections (Fig 5A), suggesting
289 enhanced humoral responses in this background. Within the spleen, both susceptible
290 C57BL/6J and resistant A/J mice produced similar frequencies of memory B cell CD73+
291 FCRL5- and atypical memory CD73+ FCRL5+ CD80+ populations during infection (not
292 shown), however in A/J mice these compartments were drastically increased in their class-
293 switch recombination frequencies during secondary infection (Fig 5B). The enhanced
294 class switch potential of resistant mice was also observed in B-1 cells. Within the
295 peritoneal B-1 cell compartment (CD19+ B220^{int} CD11b+) increased percentages of CD5-
296 B-1b cells were observed during secondary infection in A/J mice, which appear to have
297 downregulated their BCR as evidenced by being IgM^{lo} (Fig 6A-B). To further validate these

298 findings, frequencies of class switched IgM-IgD- CD5+ (B-1a) or CD5- (B-1b) cells within
299 the CD43+ B-1 cell compartments of the peritoneum (not shown) and spleen were
300 determined, and a similar trend was observed (Fig 6C). Following infection, B-1 cells in
301 the spleens of A/J mice maintained high levels of BAFFR and TACI expression and
302 expressed higher levels of surface CD138 relative to C57BL/6J mice (Fig 6D-E), markers
303 known to be induced by *Nfkbid* and important for B cell activation and differentiation into
304 antibody secreting cells (Khoenkhoen et al., 2019). In addition to differences in humoral
305 immunity, an increase in peritoneal CD8 T cell in vitro recall production of IFNγ was noted
306 in A/J relative to C57BL/6J mice, however other parameters, including granzyme B and
307 IL-2 expression and CD4 T cell responses were similar (Fig S6). Collectively these data
308 suggest that while CD8 T cell production of IFNγ is enhanced in resistant mice, and likely
309 contributes to their resistance, B-2 and B-1 cells participate in a strikingly enhanced
310 humoral response in A/J mice, offering insight into how immunity against parasitic
311 infections may be achieved.

312 **B-1 cells in resistant A/J mice have enhanced germline transcription of *Ighg***
313 **constant regions, class switch recombination and different activation profiles**

314 The diminished antibody response in bumble mice as well as the B cell phenotypic
315 differences noted in A/J mice prompted us to investigate further how *Nfkbid* may be
316 modulating the B cell compartment in both genetic backgrounds. A transcriptomic
317 approach was taken to define peritoneal B-1a, B-1b and B-2 cell response characteristics
318 in resistant and susceptible mice during naïve, chronic and secondary infection states
319 (Dataset S2). GO term enrichment analysis consistently found type I and II interferon
320 signaling and immune defense signatures as being enriched in the most differentially
321 regulated genes among B cells following infection irrespective of genetic background (Fig
322 S7A, not shown). Looking specifically at CD5- B-1b cells in A/J mice, which bore evidence

323 for enhanced activation (Fig 6), pathway enrichment analysis of genes differentially
324 upregulated on day 5 of secondary infection compared to the naïve state found additional
325 signatures of TLR-signaling, complement activation and somatic recombination (Fig S7A).
326 Germline transcription of *Ighg1*, *Ighg3*, *Ighg2b*, and *Ighg2a/c* was greatly enhanced in
327 CD5- B-1b cells from A/J compared to C57BL/6J mice on day 5 of secondary infection
328 (Fig 6F), suggesting heightened isotype class switching occurred in mice on the resistant
329 background. Consistent with their IgM-IgD- phenotype (Fig 6B 6C), both B-1a and B-1b
330 cells underwent significant IgG isotype class-switching as revealed by intracellular
331 staining, which was readily observed in the splenic environment of A/J mice (Fig 6 G-H)
332 where activated B-1 cells migrate to secrete antibody (Ha et al., 2006; Itakura et al., 2005;
333 Waffarn et al., 2015). Moreover, *Scimp* an adaptor for TLR4 signaling (Luo et al., 2017),
334 *Semaphorin7* a noted inducer of inflammatory cytokines (Suzuki, K. et al., 2007), the
335 alarmins *S100a8* and *S100a9*, and genes associated with tissue tolerance including
336 *Retnlg* and *Slpi,* were specifically upregulated in CD5- B-1b cells from A/J compared to
337 C57BL/6 mice on day 5 of challenge (Fig S7B). Gene Set Enrichment Analysis (GSEA) of
338 CD5- B-1b transcriptional variation between mice on day 5 of challenge detected
339 correlation with gene sets that distinguish B cells following vaccination with different TLR-
340 stimulating adjuvants (MPL vs R848, GSE25677) (Fig S7C). In summary, the
341 transcriptomics data suggest in the resistant A/J background, but not in C57BL/6J mice,
342 B-1 cells undergo Ig class switch recombination, perhaps through enhanced TLR-
343 signaling.

344 **Gene dosage of *Nfkbid* impacts parasite-specific IgG1 responses**

345 Because A/J *Nfkbid* polymorphisms are largely found in non-coding regions
346 (Dataset S1), we hypothesized that B cell differences observed in our system could be
347 due to differences in *Nfkbid* expression levels. To investigate this possibility, we quantified

348 *Nfkbid* expression within our transcriptomic dataset as well as by qPCR. B cells from
349 C57BL/6J mice had greater expression of *Nfkbid* relative to A/J, particularly at the chronic
350 infection stage (Fig 7A). Because *Nfkbid* expression differences could reflect heightened
351 responsiveness to parasite load, we stimulated enriched peritoneal and splenic B cells
352 from A/J and C57BL/6J mice with LPS and noted that B cells from C57BL/6J mice had on
353 average 1.5- to 2-fold greater induction of *Nfkbid* transcripts relative to A/J (Fig 7B).

354 To explore how gene dosage of *Nfkbid* impacts antibody responses generated
355 against *T. gondii,* serum from chronically infected bumble heterozygotes (*Nfkbid*+/-),
356 C57BL/6J, and A/J mice were analyzed. Although parasite-specific IgM and IgG3 did not
357 differ between mouse strains (not shown), increased parasite-specific IgG1 serum
358 responses were observed in A/J relative to C57BL/6 mice, a response that was
359 phenocopied for IgG1 in bumble heterozygotes (Fig 7C-D). The increase in IgG1 was also
360 reflected in CD138+ plasma cell differentiation in the bumble heterozygotes (Fig 7E-F),
361 consistent with previous reports that *Nfkbid* regulates plasma blast and IgG1 responses
362 (Hosokawa et al., 2017; Khoenkhoen et al., 2019; Touma et al., 2011). Hence, while
363 *Nfkbid* is required for the generation of IgM and robust IgG responses against *T. gondii*,
364 gene dosage of *Nfkbid* further controls IgG1 isotype profiles, presenting *Nfkbid* as tunable
365 modulator of antibody IgG responses to parasites. Of note, when *Nfkbid+/-* mice were
366 given secondary infections with the GT1 strain, all mice succumbed to the challenge (not
367 shown), observations that are consistent with a multiple-QTL model for *T. gondii* immunity
368 and apparent need for additional modifiers on chromosomes 10 and 17 to survive highly
369 virulent challenges.

370

371 **DISCUSSION**

372 The findings of this study underscore the utility of using inbred mouse panels to
373 uncover novel determinants of immunity to parasites. An unbiased genetic screen
374 identified *Nfkbid*, a tunable regulator of humoral responses to parasites. Within the
375 C57BL/6J background, *Nfkbid* is required for maturation and class switching of B-2 cells
376 during chronic *T. gondii* infection. While B-2 responses dominate the antibody response
377 in this background, the lack of B-1 cells appear partially responsible for the immunity defect
378 observed in bumble and are required for immunity in bone marrow chimeric mice. In
379 contrast, survival against *T. gondii* infection in resistant mice correlates with a strong
380 layered humoral response: enhanced activation and class-switching in both B-1 and B-2
381 cells. In this context, B-1 cells may assist the B-2 response to provide full immunity to
382 challenge. The ability of B-1 cells to make parasite-specific antibodies, though of lower
383 affinity, potentially amplifies B-2 immune responses to *T. gondii* through internalization of
384 B-1 cell-derived antigen-antibody complexes (Nguyen et al., 2017), assisting MHCII
385 antigen presentation for CD4 T cell help (Blandino and Baumgarth, 2019). Moreover, the
386 effect of B cell-mediated immunity to *T. gondii* and other pathogens is likely
387 underestimated in murine models using the C57BL/6 background, as enhanced B-1 and
388 B-2 responses were primarily observed in A/J mice.

389 Though the exact pathway remains to be investigated, *Nfkbid* is downstream of
390 TLR signaling in B cells (Arnold et al., 2012; Khoenkhoen et al., 2019; Touma et al., 2011),
391 which in B-1a cells causes them to downregulate CD5 and facilitate differentiation into
392 antibody secreting cells (Kreuk et al., 2019; Savage et al., 2019). CD5 is a potent negative
393 regulator of antigen receptor signaling that renders B-1a cells unresponsive to B cell
394 receptor (BCR)-triggering. This inhibition is overcome by TLR-stimulation which causes
395 CD5 to dissociate with the BCR, thereby releasing repression of BCR-mediated signaling
396 and antibody secretion (Savage et al., 2019) against foreign- and self-antigen (Kreuk et

397 al., 2019). These data suggest CD5- B-1b cells may represent an activated state of B-1
398 cells, and calls into question a strict division of labor between these two subsets. This
399 supposition would fit several of the observations made in our system, including evidence
400 for enhanced class switch recombination and TLR-gene signatures observed in the CD5-
401 B-1 cells of the resistant background. In addition, BAFFR and TACI are known inducers
402 of class-switch recombination (Castigli et al., 2005), and increased expression of these
403 receptors may further lower the threshold of activation and differentiation into CD138+
404 plasmablasts/plasma cells, all of which are regulated by *Nfkbid* (Khoenkhoen et al., 2019)
405 and occurring with greater magnitude in B-1 cells of genetically resistant A/J mice.
406 Although class switch recombination occurs with much greater frequency in B-2 cells of
407 A/J mice, we found no evidence for enhanced expression of BAFFR and TACI in this
408 compartment following *T. gondii* infection (not shown). Further investigation of pathways
409 upstream of *Nfkbid* has the potential to elucidate key requirements for *T. gondii* immunity.
410 *Nfkbid* appears to regulate transitional development in B-2 cells, which is
411 analogous to previous findings in B-1 cells (Pedersen et al., 2014), but only evident
412 following *T. gondii* infection. As immature B cells migrate out of the bone marrow to the
413 spleen, there are several checkpoints which are controlled by NF-κB such as BCR- or
414 BAFF-mediated signaling (Rowland et al., 2010), both of which are regulated by *Nfkbid*
415 (Khoenkhoen et al., 2019). Our observation of an accumulation of transitional B cells
416 during *T. gondii* infection in bumble mice suggest *Nfkbid* plays a role in stabilizing
417 advancement out of these developmental checkpoints. *Nfkbid* could act as a negative
418 regulator of BCR signaling, enabling pathogen-reactive B-2 cells to develop beyond
419 negative selection that would otherwise occur as antigen accumulates in secondary
420 lymphoid organs over time. Alternatively, *Nfkbid* could be a positive regulator of NF-κB
421 signaling, increasing the strength of BCR signaling to enable transitional B cells to become

422 mature B cells. In both cases, a developmental defect likely restricts the pool of *T. gondii*-
423 reactive mature B cells, preventing replenishment of antibody secreting cells during
424 infection, culminating in the low parasite-specific antibody titers observed in bumble mice.
425 It is important to emphasize that multiple polymorphisms determine the complex
426 phenotype of secondary infection immunity to *T. gondii*. Our genetic screen revealed at
427 least 4 loci that each account for 20-40% of the overall heterologous immunity to *T. gondii*,
428 and that the H-2 locus can be an important modifier of resistance against certain parasite
429 strains. Perhaps not surprising, the *Nfkbid* polymorphism in a stand-alone fashion did not
430 fully restore immunity, as inferred from chromosome 7 consomic mice and by our attempts
431 to mimic the lower gene expression observed in resistant mice through heterozygous
432 expression. Whereas polymorphic *Nfkbid* contributes 21% to this phenotype, perhaps by
433 regulating plasma cell differentiation (Fig 7), this smaller effect QTL was instrumental in
434 identifying *Nfkbid*, where a more drastic gene inactivation revealed its role in multiple
435 compartments in bumble mice, notwithstanding its requirement for humoral immunity.
436 In summary, heterologous immunity to a parasitic pathogen should, at a minimum,
437 prevent disease against a wide variety of strains that differ in virulence or polymorphic
438 antigens. An ideal parasite vaccine would entirely protect against re-infection and induce
439 sterile immunity, thought possible since re-infection studies were first performed in mice
440 (Nussenzweig et al., 1967) and humans immunized with irradiated sporozoites and
441 *Plasmodium sp.* challenge (Hoffman et al., 2002). Yet, only one partially protective vaccine
442 is in use for any human parasitic pathogen, RTS,S/AS01, which has low efficacy for
443 malaria prevention (RTS, S Clinical Trials Partnership, 2015). Our findings highlight the
444 role of both innate and conventional B cells in humoral immunity to *T. gondii*, introducing
445 B-1 cells as a potential vaccine target along with B-2 cells to maximize humoral immunity
446 to parasitic infections. Moreover, we present a modulator of antibody responses against

447 parasitic infections, *Nfkbid*, a transcriptional regulator that can tune B cell responses to
448 provide an overall effective class-switched antibody response against parasites.
449

450 **ACKNOWLEDGMENTS**

451 This work was supported by NIH grants R01 AI137126, R15 AI131027, a Hellmann
452 Fellowship and an MCB departmental award to KJ; and by NIH grants U19-AI109962 and
453 R01 AI117890 to NB. The sequencing was carried out at the DNA Technologies and
454 Expression Analysis Cores at the UC Davis Genome Center, supported by NIH Shared
455 Instrumentation Grant 1S10OD010786-01. We would like to thank David Gravano and the
456 UC Merced Stem Cell Instrumentation Foundry for their assistance designing panels and
457 utilizing instruments, supported by the DoD Research and Education Program for
458 HBCU/MSI Instrumentation Grant W911NF1910529. The authors declare no conflict of
459 interest.
460
461 **Author Contributions:** S.P.S., S.D.S., N.B. and K.J. designed research; S.P.S., S.D.S.,
462 J.A., J.C.S.A., J.W., S.W., and K.J. performed research; Z.L. and N.B. contributed new
463 reagents/analytic tools; S.P.S., S.D.S., and K.J. analyzed data; and S.P.S., S.D.S., N.B.
464 and K.J. wrote the paper.
465 **Competing Interest Statement:** The authors disclose no competing interests.
466

467 **FIGURES AND TABLES**

468

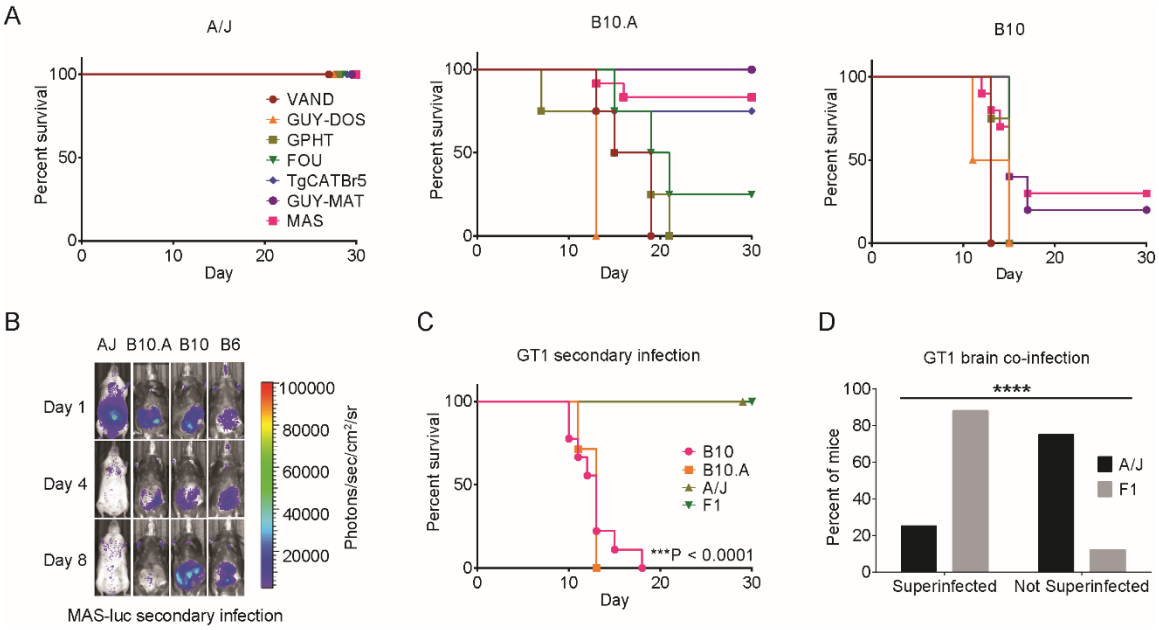

469

470 **Figure 1. MHC and non-MHC alleles promote immunity to virulent *Toxoplasma***

471 ***gondii* strains in A/J mice.**

472 All mice were infected with 10^4 type III CEP *hxgprt-* avirulent *T. gondii* parasites and

473 allowed to progress to chronic infection; then, 35 days later, mice were challenged with

474 $5x10^4$ of the indicated strains of *T. gondii*. A) Survival of A/J, C57BL/10J (B10), and

475 C57BL/10J.A (B10.A) mice following secondary infection with atypical strains of *T. gondii*.

476 Cumulative results are plotted from 1-2 experiments; n=4 to 12 mice per parasite strain

477 and mouse genetic background. B) Bioluminescence imaging of individual mice

478 challenged with luciferase expressing MAS strain on days 1, 4 and 8 of secondary

479 infection; parasite burden is shown as a heat map depicting the relative number of photons

480 (photons/sec/cm2/sr) detected over a 5 minute exposure. C) Survival of B10 (n=5), B10.A

481 (n=5), A/J (n=12), and F1 (A/J x C57BL/6, n=9) mice following secondary infection with

482 the type I GT1 strain; ***P<0.0001, Log-rank (Mantel-Cox) compared to A/J mice.

483 Cumulative data from 1 to 2 experiments are plotted. D) Superinfection in surviving A/J

484 (n=12) and F1 (n=9) mice following 35 days of secondary infection with the type I GT1
485 strain. To evaluate superinfection, brain homogenate was grown in MPA-xanthine
486 selection medium, which selects for GT1 parasites expressing the endogenous *HXGPRT*
487 locus and against the *hxgprt-* type III CEP strain used to induce chronic infection. Plotted
488 is the fraction of mice for which the presence or absence of the GT1 strain was detected;
489 **** P< 0.0001, Fisher's exact test.

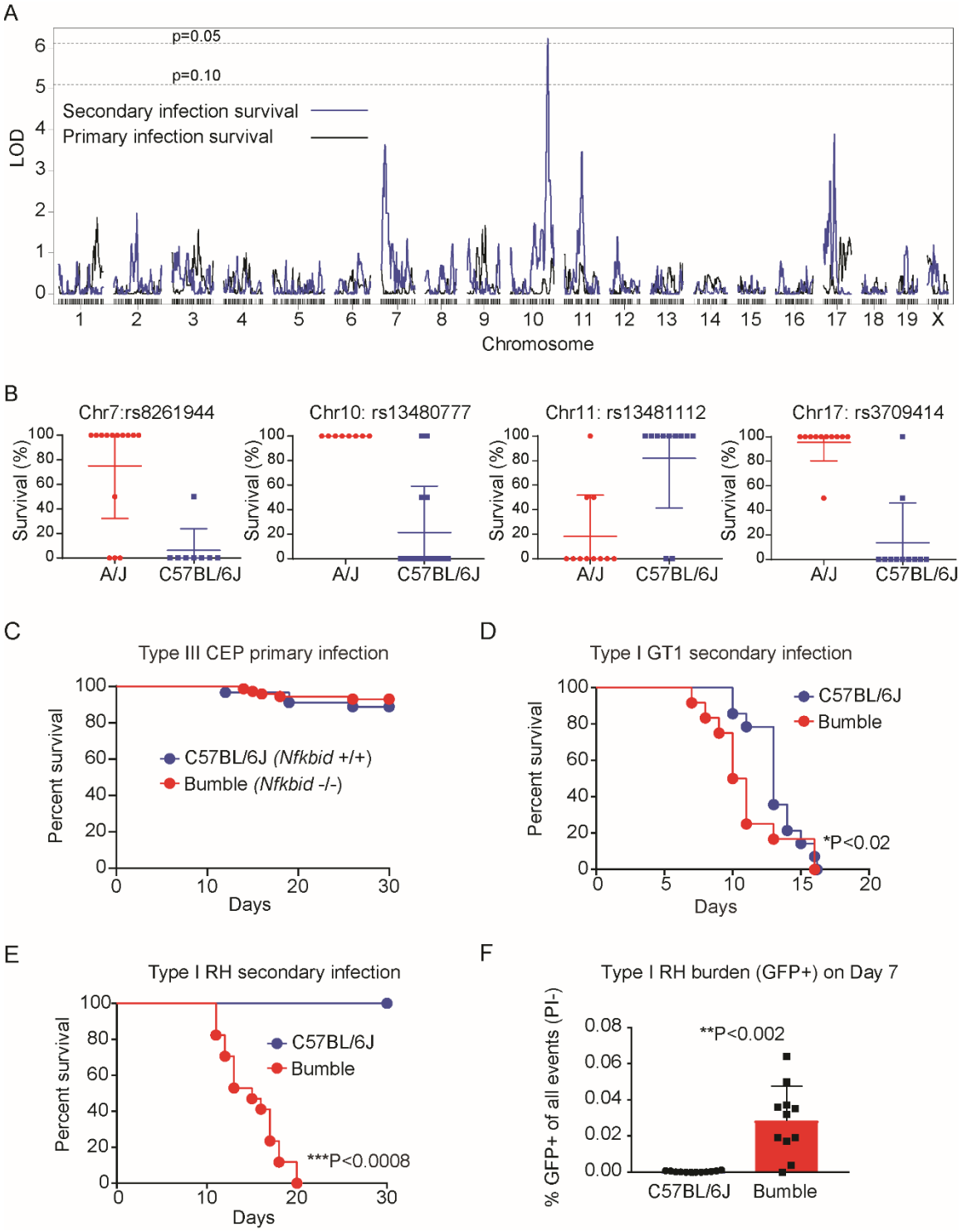
A
p=0.05
p=0.10
Secondary infection survival
Primary infection survival
LOD
Chromosome
B
Chr7:rs8261944
Chr10: rs13480777
Chr11: rs13481112
Chr17: rs3709414
Survival (%)
A/J
C57BL/6J
C
Type III CEP primary infection
Percent survival
C57BL/6J (Nfkbid +/+)
Bumble (Nfkbid -/-)
Days
D
Type I GT1 secondary infection
C57BL/6J
Bumble
*P<0.02
E
Type I RH secondary infection
***P<0.0008
F
Type I RH burden (GFP+) on Day 7
% GFP+ of all events (PI-)
**P<0.002

494 **Figure 2. Genetic mapping reveals *Nfkbid* is required for immunity to *Toxoplasma***
495 ***gondii* secondary infections.**
496 26 recombinant inbred (RI) mouse strains from the AxB;BxA panel were primed with 10^4
497 type III *T. gondii* CEP *hxgprt-* parasites; then, 35 days later, mice were challenged with
498 $5x10^4$ virulent type I GT1 *T. gondii* parasites (n=2 per RI line). A) LOD scores for each
499 marker were calculated using Haley-Knott regression and the running LOD scores of
500 primary (black) and secondary infection survival (blue) for each genetic marker is plotted.
501 1000 permutations were performed to obtain the genome wide threshold LOD values;
502 P=0.10 and 0.05 thresholds are shown. B) Effect plots for the genetic markers closest to
503 the maximal LOD scores calculated for the chromosome 7, 10, 11 and 17 QTLs are shown.
504 Each dot indicates the percent survival of a unique RI line and whether it encodes an A/J
505 (red) or C57BL/6 (blue) allele at the specified genetic marker. C) Cumulative survival of
506 bumble (*Nfkbid*-/- C57BL/6) (n=71) and wildtype (C57BL/6J) (n=89) naïve mice infected
507 with the avirulent type III CEP strain. D) Survival of chronically infected bumble (n=12) and
508 wildtype (n=8) mice given a secondary infection with the type I GT1 strain. Cumulative
509 survival from 3 separate experiments are shown; * P<0.02, Gehan-Breslow-Wilcoxon test.
510 E) As in B, but survival to secondary infection with the type I RH strain is shown.
511 Cumulative survival from 3 separate experiments is plotted (bumble n=17, C57BL/6J n=4);
512 ***P<0.008, Mantel-Cox test. F) Frequency of GFP+ events in the peritoneal lavage 7 days
513 post-secondary infection with GFP-expressing type 1 RH strain (RH 1-1). Each dot
514 represents the result of one mouse, and cumulative results are shown from 3 separate
515 experiments (bumble n=13, C57BL/6J n=17); **P<0.002, unpaired two-tailed t-test.
516

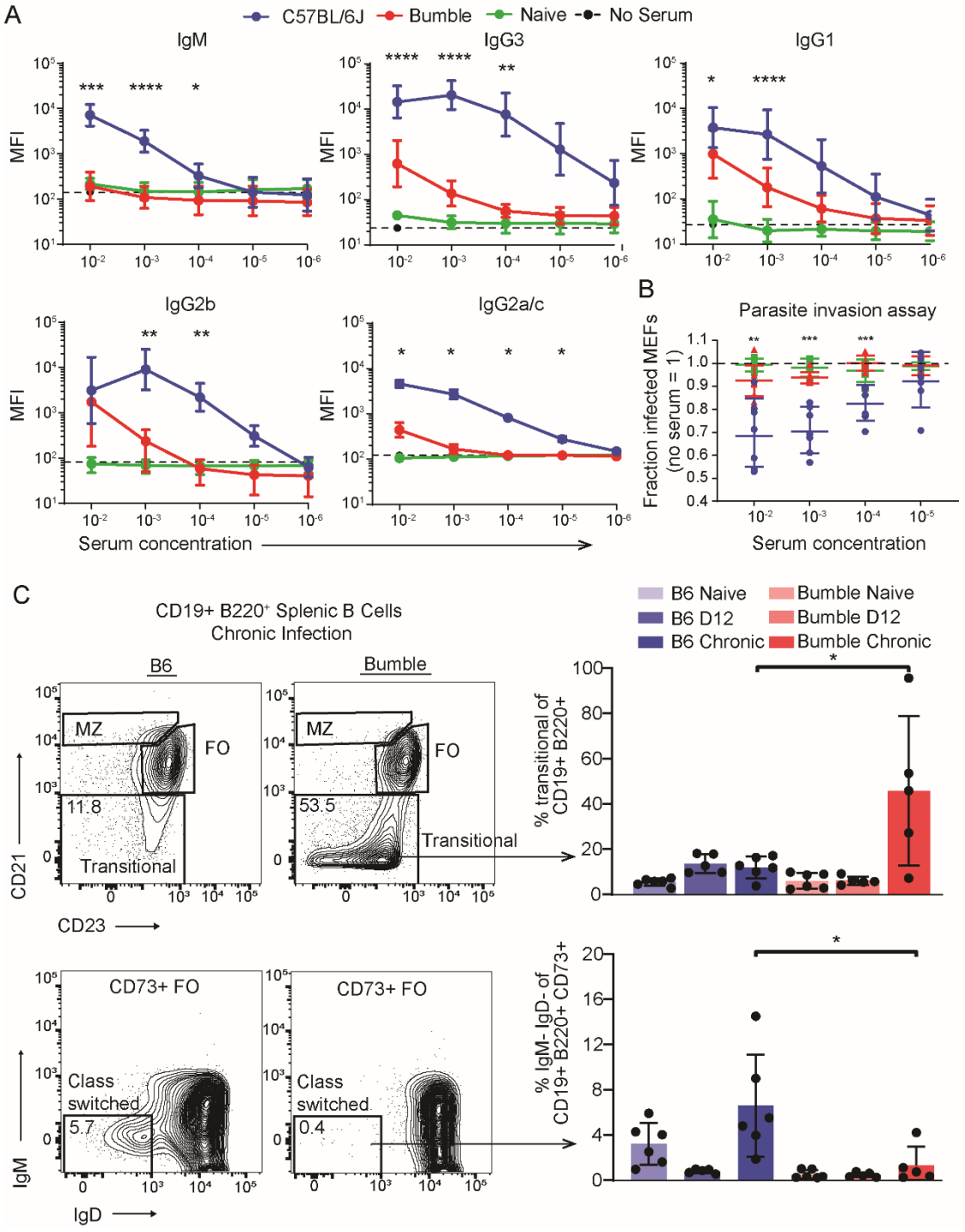
A
C57BL/6J
Bumble
Naive
No Serum
IgM
IgG3
IgG1
IgG2b
IgG2a/c
MFI
Serum concentration
B
Parasite invasion assay
Fraction infected MEFs (no serum = 1)
Serum concentration
C
CD19+ B220+ Splenic B Cells
Chronic Infection
B6
Bumble
MZ
FO
11.8
53.5
Transitional
CD21
CD23
B6 Naive
B6 D12
B6 Chronic
Bumble Naive
Bumble D12
Bumble Chronic
% transitional of CD19+ B220+
CD73+ FO
Class switched
5.7
0.4
IgM
IgD
% IgM- IgD- of CD19+ B220+ CD73+

517

518 **Figure 3. *Nfkbid* is required for humoral responses to *Toxoplasma gondii*.**

519 A) Whole fixed GFP+ parasites were incubated with serum from chronically infected mice,
520 stained with fluorescently labeled anti-isotype antibodies and assessed by flow cytometry.
521 Quantification of *T. gondii*-specific antibody isotype binding (IgM, IgG1, IgG2a/c, IgG2b,
522 and IgG3) over a range of serum concentrations is shown. Background staining in the
523 absence of serum is indicated by the dotted line for each isotype. Plotted is the cumulative
524 average +/-SD of the geometric mean fluorescence straining intensity (MFI) from 3
525 separate experiments (bumble n=8, C57BL/6J n=11). B) Neutralization of GFP+ parasites
526 coated with serum over a range of concentrations from the indicated chronically infected
527 mice. Parasites were incubated in serum for 20 minutes before infection of mouse
528 embryonic fibroblasts and assessed by FACS 2h later. The fraction of infected host cells
529 (GFP+ cells) is normalized to that of parasite infections without serum. Each dot
530 represents the serum from an individual mouse and cumulative results from 3 separate
531 experiments are shown (bumble n=8, C57BL/6J n=7, naïve n=6). For A and B, significance
532 was assessed by unpaired t-tests with Holm-Sidak correction for multiple comparisons;
533 *** P< 0.001, ** P<0.01, * P<0.01. C) Representative FACS plots of chronically infected
534 bumble and B6 mice and scatter plot of the frequency of splenic B-2 cell compartments
535 quantifying transitional B cells at naïve, d12 of primary infection, and chronic infection.
536 Representative FACS plots of chronically infected bumble and B6 mice and scatter plot of
537 the frequency of IgM- IgD- cells of the CD73+ conventional memory B population.
538 Cumulative data from two experiments n=5-6 mice/condition. * P<0.05 by unpaired two-
539 tailed t-test.

540

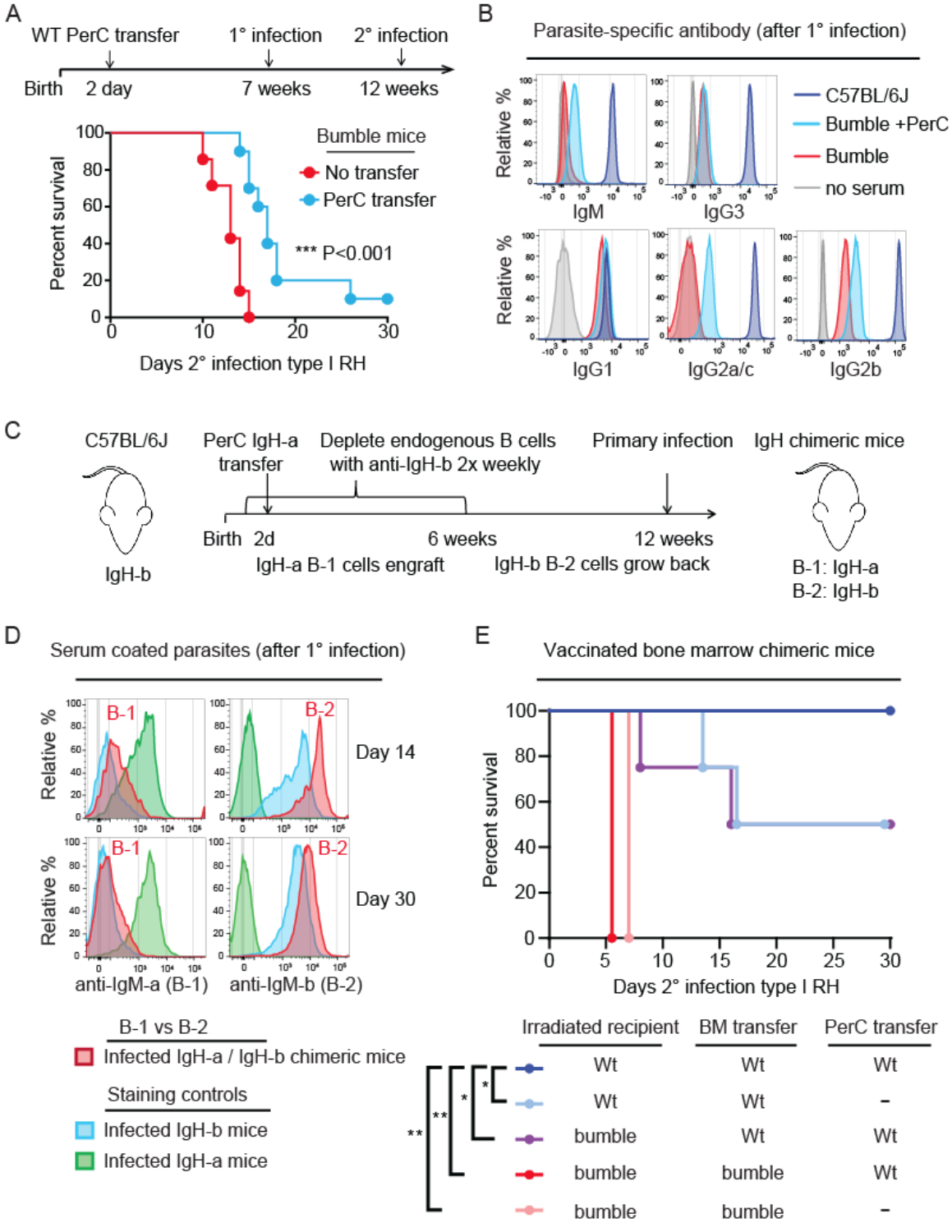
A
WT PerC transfer
1° infection
2° infection
Birth
2 day
7 weeks
12 weeks
Percent survival
Bumble mice
No transfer
PerC transfer
*** P<0.001
Days 2° infection type I RH
B
Parasite-specific antibody (after 1° infection)
Relative %
IgM
IgG3
IgG1
IgG2a/c
IgG2b
C57BL/6J
Bumble +PerC
Bumble
no serum
C
C57BL/6J
IgH-b
PerC IgH-a transfer
Deplete endogenous B cells with anti-IgH-b 2x weekly
Primary infection
IgH chimeric mice
Birth
2d
6 weeks
12 weeks
IgH-a B-1 cells engraft
IgH-b B-2 cells grow back
B-1: IgH-a
B-2: IgH-b
D
Serum coated parasites (after 1° infection)
B-1
B-2
Day 14
Day 30
anti-IgM-a (B-1)
anti-IgM-b (B-2)
E
Vaccinated bone marrow chimeric mice
Percent survival
Days 2° infection type I RH
B-1 vs B-2
Infected IgH-a / IgH-b chimeric mice
Staining controls
Infected IgH-b mice
Infected IgH-a mice
Irradiated recipient
BM transfer
PerC transfer
Wt
Wt
Wt
Wt
Wt
-
bumble
Wt
Wt
bumble
bumble
Wt
bumble
bumble
-

541

542 **Figure 4. The contribution of B-1 and B-2 cells to *Toxoplasma gondii* immunity in**
543 **C57BL/6J mice.**

544 A) Schematic of the secondary infection experiment using PerC reconstituted bumble
545 mice. 2-4 day old bumble neonates were transferred $5x10^6$ total PerC and allowed to rest
546 for 7 weeks before primary infection with the type III CEP strain. 5 weeks post-primary
547 infection, mice were given a secondary infection with the type I strain RH. Survival of
548 bumble mice given total PerC transfers (n=10) relative to littermate controls (n=12).
549 Cumulative survival is shown from 3 separate experiments; *** P <0.001, Mantel-Cox test.
550 B) Representative histograms of anti-isotype staining of parasites coated in serum (10^3
551 dilution for IgG, 10^2 for IgM) from chronically infected bumble, bumble given PerC transfer,
552 and WT mice. C) Schematic of neonatal allotype chimera generation. C57BL/6J neonates
553 were given anti-IgHb to deplete endogenous B cells at day 1 post birth and twice weekly
554 after for 6 weeks, thereby depleting the endogenous B-1 pool for the life of the animal due
555 to their restricted fetal/neonatal window of development. Neonates were given $5x10^6$ total
556 PerC from 6-8 week old IgH-a congenic C57BL/6 mice donors. These mice then rested
557 for 6 weeks after the last depletion treatment to allow reemergence of the endogenous B-
558 2 IgH-b cells. D) Representative histograms of serum derived anti-IgM-a (B-1 derived) or
559 anti-IgM-b (B-2 derived) staining profiles of type I RH GFP+ parasites taken from the IgH
560 allotype chimeras on day 14 and 30 following primary type III CEP infection. Staining
561 controls with serum from chronically infected C57BL/6J IgH-b littermates, or IgH-a mice
562 are shown. E) Irradiated bumble and WT recipients (45.1 or 45.2) were given WT or
563 bumble bone marrow (BM) with or without total WT PerC (45.2). Mice were vaccinated
564 with a replication deficient type I strain (RH *Δup Δompdc*) and 30d later challenged with

565 type I RH. Cumulative survival is shown from 2-3 experiments (n=4-9 per condition); *

566 P<0.05 by Mantel-Cox test.

567

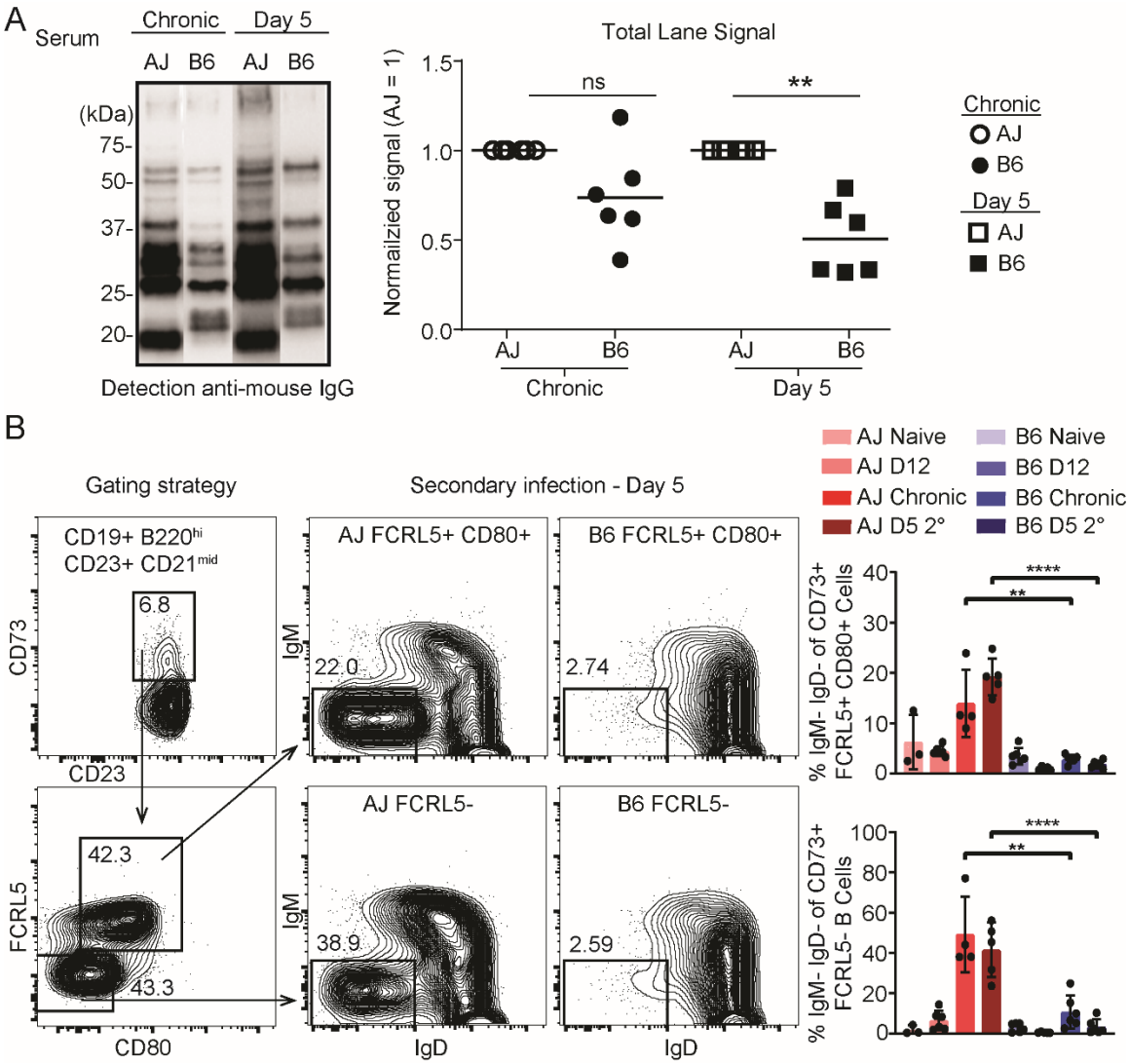

Figure 5. Immunity in A/J mice correlates with enhanced class-switching in memory B-2 cells and increased serum reactivity to parasite lysate antigen.

A) Serum obtained from A/J and C57BL/6J mice chronically infected (CEP) or at D5 of secondary infection (GT1) were used to probe GT1 parasite lysate separated by SDS-PAGE, western blots were detected with anti-mouse IgG. “Total Lane Signal” is the signal obtained from the entire lane of C57BL/6J compared to that of A/J (=1); western blots were developed in tandem and analyzed by Image J. Results are from 6 individual experiments; ** $P < 0.01$, * $P < 0.05$; unpaired two-tailed t-tests. B) Gating strategies for identifying

577 memory B cells. Memory B cells are identified as CD19+ B220+ CD23+ CD21^{mid} CD73+.
578 Conventional memory B cells are FCRL5- CD80- while atypical memory B cells are
579 identified as FCRL5+, CD80+. Representative FACS plots of memory compartments in
580 A/J and C57BL/6J mice on day 5 of secondary infection with the type I GT1 strain are
581 shown. The frequency of class-switched (IgM- IgD-) memory cells at the indicated infection
582 states were analyzed. Each dot represents the results from an individual mouse and the
583 cumulative averages +SD from 2 experiments are plotted. N=3-6 mice per infection state.
584 Significance was assessed with an unpaired two-tailed t-test; *** P<0.0001, ** P<0.01.
585

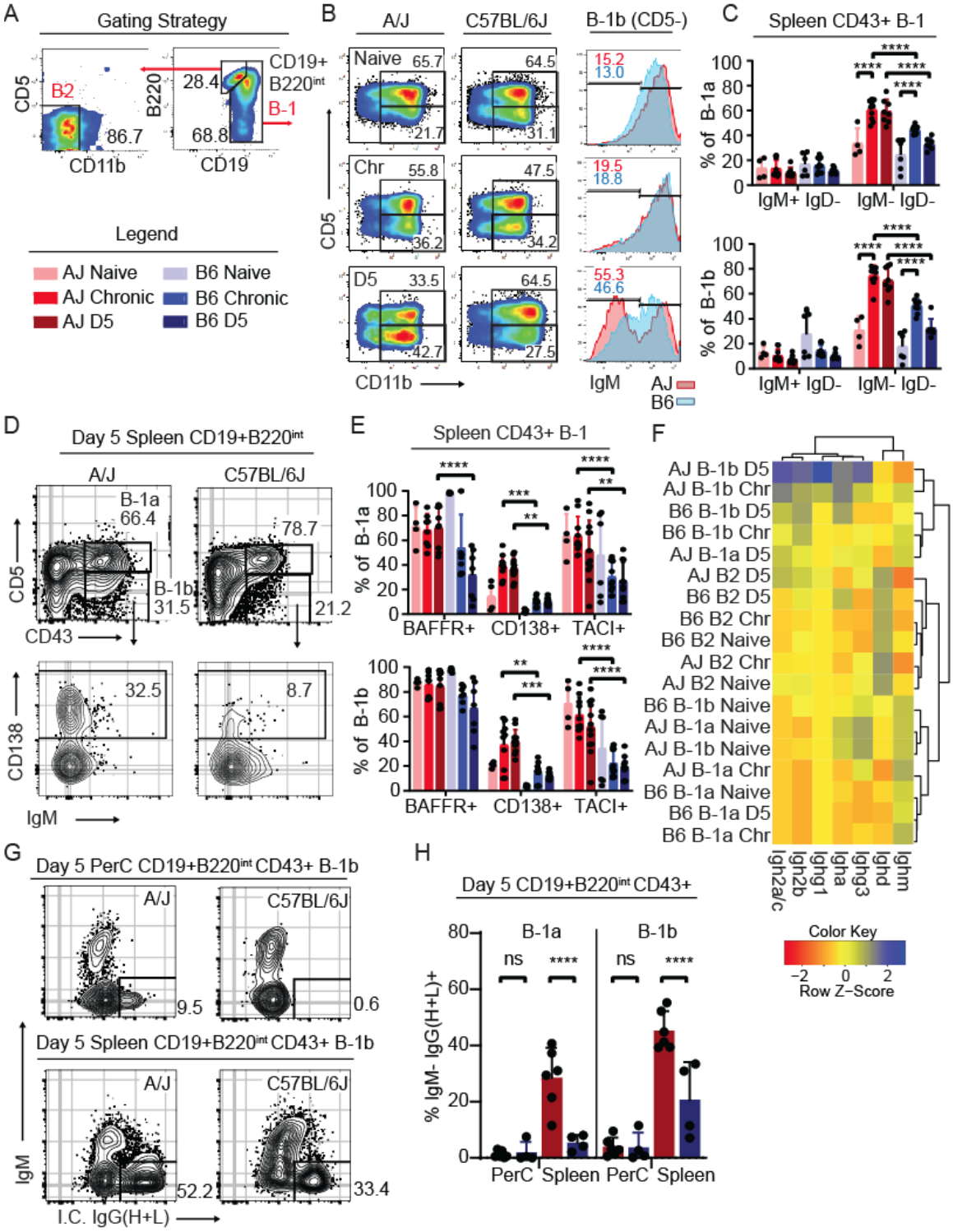
A
Gating Strategy
CD5
B2
86.7
CD11b
B220
28.4
68.8
CD19
CD19+
B220int
B-1
Legend
AJ Naive
AJ Chronic
AJ D5
B6 Naive
B6 Chronic
B6 D5
B
A/J
C57BL/6J
B-1b (CD5-)
Naive
65.7
21.7
64.5
31.1
15.2
13.0
Chr
55.8
36.2
47.5
34.2
19.5
18.8
D5
33.5
42.7
64.5
27.5
55.3
46.6
CD5
CD11b
IgM
AJ
B6
C
Spleen CD43+ B-1
% of B-1a
% of B-1b
IgM+ IgD-
IgM- IgD-
D
Day 5 Spleen CD19+B220int
A/J
C57BL/6J
B-1a
66.4
78.7
B-1b
31.5
21.2
CD5
CD43
32.5
8.7
CD138
IgM
E
Spleen CD43+ B-1
% of B-1a
% of B-1b
BAFFR+
CD138+
TACI+
F
AJ B-1b D5
AJ B-1b Chr
B6 B-1b D5
B6 B-1b Chr
AJ B-1a D5
AJ B2 D5
B6 B2 D5
B6 B2 Chr
B6 B2 Naive
AJ B2 Chr
AJ B2 Naive
B6 B-1b Naive
AJ B-1a Naive
AJ B-1b Naive
AJ B-1a Chr
B6 B-1a Naive
B6 B-1a D5
B6 B-1a Chr
Igh2a/c
Igh2b
Ighg1
Ighg3
Ighd
Ighm
Color Key
−2
0
2
Row Z−Score
G
Day 5 PerC CD19+B220int CD43+ B-1b
A/J
C57BL/6J
9.5
0.6
Day 5 Spleen CD19+B220int CD43+ B-1b
52.2
33.4
IgM
I.C. IgG(H+L)
H
Day 5 CD19+B220int CD43+
B-1a
B-1b
ns
% IgM- IgG(H+L)+
PerC
Spleen

586

587

588 **Figure 6. Evidence for enhanced B-1 cell activation in resistant A/J mice.**

589 A) Gating strategies for identifying B-1 (CD19+ B220$^{int-neg}$) and B-2 (CD19+ B220^{hi}) B cells.
590 The legend applies to panels C-H. B) Representative FACS plots of the CD11b+ peritoneal
591 B-1 B cell compartment in A/J and C57BL/6J (B6) mice at naïve, chronic (Chr), and 5 days
592 (D5) post-secondary infection with the GT1 strain. Numbers indicate the percent of cells
593 that fall within the indicated gate. Representative histograms of IgM surface expression
594 and percent of cells that fall within the IgM^{lo} gate of CD5- B-1b cells from A/J (red) and
595 C57BL/6J (blue) at the indicated time points. C) Frequencies of splenic CD43+ B-1a
596 (CD5+) or B-1b (CD5-) that are IgM+IgD- or IgM-IgD- in A/J and C57BL/6J mice at the
597 indicated infection states. D) Representative FACS plots of splenic CD19+ B220$^{int-neg}$ B
598 cells stained for CD43 and CD5 in A/J and C57BL/6J mice at D5 of secondary infection.
599 Representative CD138 expression on CD5- CD43+ B-1b cells. E) Frequencies of CD43+
600 splenic B-1a and B-1b cells from A/J and C57BL/6J mice that express BAFFR+, TACI+,
601 or CD138+ at the indicated infection states. F) Heatmap depicting the relative expression
602 of all *Ighg* transcripts from the indicated B cell population, mouse strain and infection state.
603 G) Representative FACS plots of intracellular IgG (H+L) of B-1b cells, and H) frequency
604 of both peritoneal and splenic B-1a and B-1b cells of A/J and C57BL/6J mice at day 5 of
605 secondary infection. For C, E and H, the cumulative average +SD from 2-4 experiments
606 is plotted and each dot represents the result from an individual mouse; P values calculated
607 by 2-way ANOVA with Tukey correction; **** $P<0.0001$, *** $P<0.001$, ** $P<0.01$, * $P<0.05$.
608

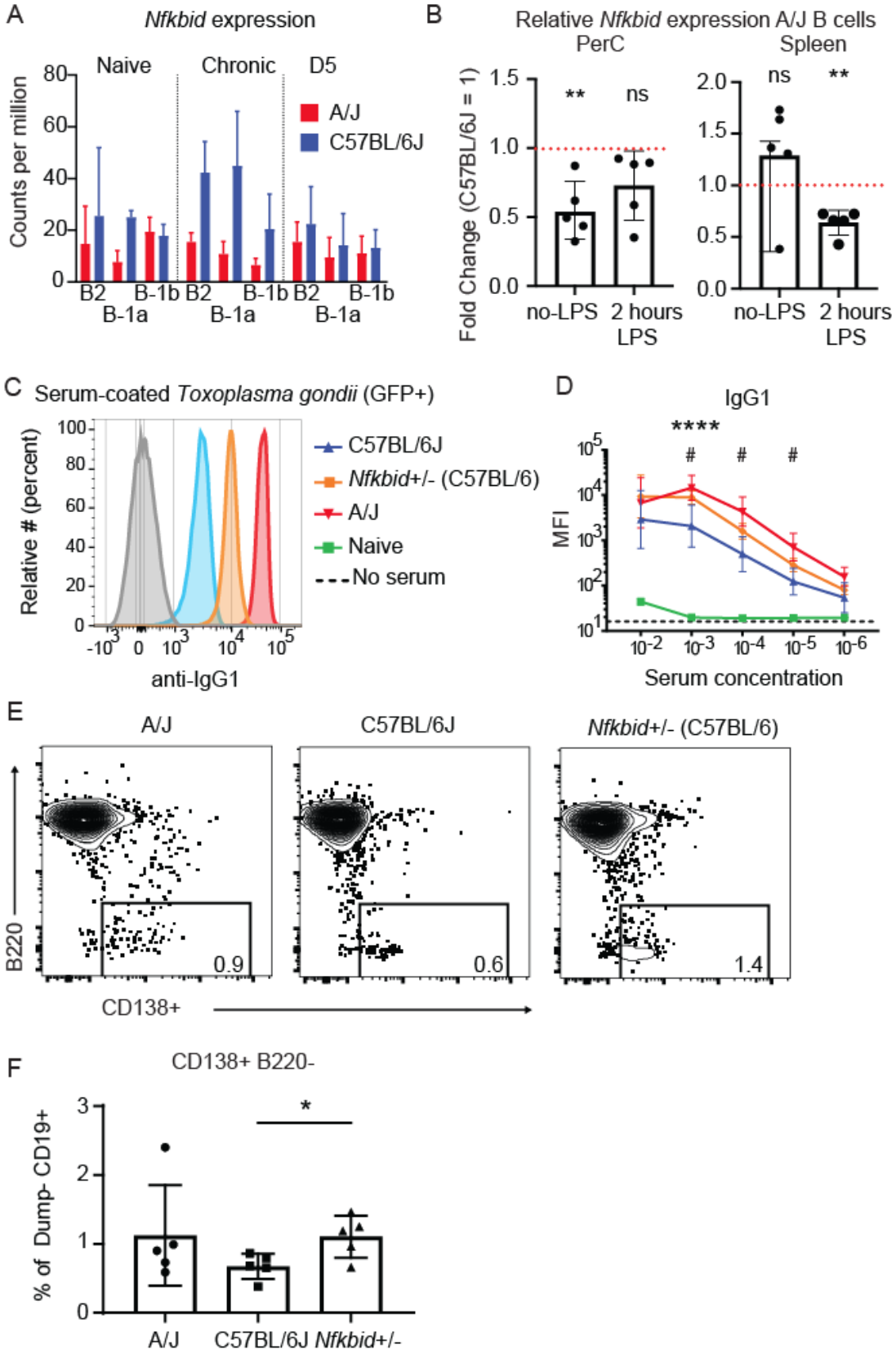
A
Nfkbid expression
Naive
Chronic
D5
Counts per million
A/J
C57BL/6J
B2
B-1b
B-1a
B
Relative Nfkbid expression A/J B cells
PerC
Spleen
Fold Change (C57BL/6J = 1)
**
ns
no-LPS
2 hours LPS
C
Serum-coated Toxoplasma gondii (GFP+)
Relative # (percent)
anti-IgG1
C57BL/6J
Nfkbid+/- (C57BL/6)
A/J
Naive
No serum
D
IgG1
****
MFI
Serum concentration
E
A/J
C57BL/6J
Nfkbid+/- (C57BL/6)
B220
CD138+
0.9
0.6
1.4
F
CD138+ B220-
% of Dump- CD19+
*
A/J
C57BL/6J
Nfkbid+/-

609

610 **Figure 7. Gene dosage of *Nfkbid* impacts parasite-specific IgG1 responses.**

611 A) *Nfkbid* expression in CPM (Counts per million) of 3'-Tag RNA-seq reads of the indicated
612 B cell populations obtained from A/J and C57BL/6J mice that were either naïve, chronically
613 infected, or on D5 of secondary infection with the type I GT1 strain. B) Enriched B cells
614 from the PerC and spleen were stimulated with LPS for 2 hrs and *Nfkbid* transcripts were
615 quantified by qPCR; ** P< 0.01, paired t-test. C) Representative histograms display the
616 detection of parasite-specific IgG1 bound to formaldehyde fixed GFP+ type I GT1
617 parasites; diluted serums (10^3) from C57BL/6J, *Nfkbid*+/- (C57BL/6J x bumble F1), and
618 A/J mice chronically infected with the type III CEP strain were assayed. Anti-mouse IgG1
619 background staining in the absence of serum is shown. D) As in C, but quantification of
620 the parasite-specific IgG1 antibody isotype binding over a range of serum concentrations
621 is shown. Plotted is the cumulative average +/-SD of the MFI from 2-3 separate
622 experiments (C57BL/6J n=8; *Nfkbid*+/- n=7; A/J n=8); significance was assessed by
623 unpaired t-tests and Holm-Sidak corrections comparing A/J vs C57BL/6J (*) or *Nfkbid+/-*
624 vs C57BL/6J (#); **** P<0.0001, # P<0.05. IgG1 staining was not significantly different
625 between A/J and *Nfkbid*+/- serums. E) Representative FACS plots of the dump- CD19+
626 CD138+ plasmablast populations within A/J, C57BL/6J and *Nfkbid*+/- mice at day 5 of
627 secondary infection with type I GT1 parasites. F) Frequency of B220- CD138+
628 plasmablasts of total live dump- CD19+ cells. Plotted is the cumulative average +/-SD of
629 2 separate experiments (n=5 per mouse strain); significance was assessed by unpaired t-
630 tests; * P< 0.05.

631

632 **STAR METHODS**

633 **Parasite strains and cell lines**

634 Human foreskin fibroblasts (HFFs) monolayers were grown in DMEM (4.5 g/L D-glucose)
635 (Life Technologies) supplemented with 2 mM L-glutamine, 20% fetal bovine serum (FBS)
636 (Omega Scientific), 1% penicillin-streptomycin, and 0.2% gentamycin (Life Technologies).
637 Mouse Embryonic Fibroblasts (MEFs) were grown in DMEM (4.5 g/L D-glucose) (Life
638 Technologies) supplemented with 10% fetal bovine serum (FBS) (Omega Scientific),
639 20mM HEPES, 1% penicillin-streptomycin, and 0.2% gentamycin (Life Technologies).
640 *Toxoplasma gondii* strains were passaged in HFFs in 'Toxo medium' (4.5 g/L D-glucose,
641 L-glutamine in DMEM supplemented with 1% FBS and 1% penicillin-streptomycin). The
642 following clonal strains were used (clonal types are indicated in parentheses): RH Δ*ku80*
643 Δ*hxgprt* (type I), RH (1-1) *GFP::cLUC* (type I), GT1 (type I), GT1 *GFP::cLuc* (type I), and
644 CEP *hxgprt*- (type III). The following atypical strains were used: MAS, MAS *GFP::cLuc*
645 (2C8) (haplogroup 'HG' HG4), GUY-MAT (HG5), FOU (HG6), GPHT (HG6), TgCATBr5
646 (HG7), GUY-DOS (HG10), and VAND (HG10). The uracil auxotroph vaccine strain, RH
647 *Δup Δompdc* (Fox and Bzik, 2010), was passaged in HFFs in medium containing 250μM
648 uracil.

649 **Generation of GFP-expressing GT1 strains**

650 GT1 parasites were transfected with linearized plasmids for parasite expression of GFP
651 and click beetle luciferase (*GFP::cLUC*), parasites were grown on HFF monolayers in T-
652 25 flasks in Toxo medium for 2 weeks. Parasites were removed from the flasks by
653 scraping; the parasites were pelleted and washed with PBS and suspended in sterile
654 FACS buffer (2% FBS in PBS). Fluorescent parasites where then sorted via fluorescence-
655 activated cell sorting (FACS) into a 96-well plate with confluent HFF monolayers. To

656 ensure single plaque formation in at least one of the wells, the sort was titrated using the
657 following parasite numbers: 100, 50, 25, 12, 6, 3, 2, and 1 for each well per row of 8.

658 **Mice and ethics statement**

659 Female C57BL/6J (H-2b), A/J (H-2a), C57BL/10SnJ (H-2b), B10.A-*H2*^{a} *H2-T18*^{a}/SgSnJ
660 (H-2a), B6AF1/J (A/J x C57BL/6J F1 progeny), B6.129S2-*Ighm*^{tm1Cgn}/J (muMT), B6.SJL-
661 *Ptprc*^{a} *Pepc*^{b}/BoyJ (CD45.1 congenic), B6.Cg-*Gpi1*^{a} *Thy1*^{a} *Igh*^{a}/J (IgH-a triple congenic
662 mice), C57BL/6J-Chr7$^{A/J}$/NaJ and C57BL/6J-Chr10$^{A/J}$/NaJ (chromosome 7 and 10
663 consomic mice), and 26 (AxB;BxA) recombinant inbred (RI) mice derived from A/J and
664 C57BL/6 founders, were purchased from Jackson Laboratories. The bumble mouse line
665 used for this research project (Arnold et al., 2012), C57BL/6J-*Nfkbid*^{m1Btlr}/Mmmh,
666 RRID:MMRRC_036725-MU, was obtained from the Mutant Mouse Resource and
667 Research Center (MMRRC) at University of Missouri, an NIH-funded strain repository, and
668 was donated to the MMRRC by Bruce Beutler, M.D., University of Texas Southwestern
669 Medical Center. Bumble mice were crossed to C57BL/6J to generate F1 bumble
670 heterozygotes (*Nfkbid*+/-).

671 Mice were maintained under specific pathogen free conditions at UC Merced.
672 Every effort was made to ensure unnecessary stress on the animals was avoided. Mouse
673 work was performed in accordance with the National Institutes of Health Guide to the Care
674 and Use of Laboratory Animals. All protocols have been reviewed and approved by UC
675 Merced's Committee on Institutional Animal Care and Use Committee. UC Merced has an
676 Animal Welfare Assurance filed with OLAW (#A4561-01), is registered with USDA (93-R-
677 0518), and the UC Merced Animal Care Program is AAALAC accredited (001318).

678 **Parasite infections**

679 Parasite injections were prepared by scraping T-25 flasks containing vacuolated HFFs
680 and sequential syringe lysis first through a 25G needed followed by a 27G needle. The

681 parasites were spun at 400 rpm for 5 min to remove debris and the supernatant was
682 transferred, followed by a spin at 1700 rpm washing with PBS. For primary infections, mice
683 were infected intraperitoneally (i.p.) with 10^4 tachyzoites of type III CEP *hxgprt-.* For some
684 experiments, mice were vaccinated i.p. with 10^6 tachyzoites of RH *Δup Δompdc.* For
685 secondary infections, mice were infected I.P. with $5x10^5$ type I parasites (RH or GT1).
686 Parasite viability of the inoculum was determined by plaque assay following i.p. infections.
687 In brief, 100 or 300 tachyzoites were plated in HFF monolayers grown in a 24-well plate
688 and 4-6 days later were counted by microscopy (4x objective).

689 **Blood plasma isolation and assessment of seroconversion**

690 All mice were assessed for sero-positivity to *T. gondii* 4-5 weeks post primary infection.
691 50μL of blood was isolated from mice in tubes containing 5μL of 0.5M EDTA on ice,
692 pelleted and the supernatant containing blood plasma was heat inactivated to denature
693 complement at 56°C for 20 minutes and then stored at -80°C. HFFs were grown on
694 coverslips and infected with GFP-expressing RH (1-1) overnight, fixed 18 hrs later with
695 3% formaldehyde (Polysciences) in PBS, washed, permeabilized and blocked with PBS
696 containing 3% bovine serum albumin Fraction V (Sigma), 0.2M Triton X-100, 0.01%
697 sodium azide, incubated with a 1:100 dilution of collected blood plasma for 2 hrs at room
698 temperature, washed with PBS, and detected with Alexa Fluor 594-labeled secondary
699 antibodies specific for mouse IgG (cat # A11032, Life Technologies). Seropositive
700 parasites were observed by immunofluorescence microscopy (Nikon Eclipse Ti-U).

701 **Brain superinfection assays and cyst enumeration**

702 Brains from chronically infected mice (CEP *hxgprt-*) that survived secondary challenge
703 were dissected, rinsed in PBS, passed through a 21G needle several times, pelleted and
704 suspended in 1mL of PBS. For rederivation, 100μL of the brain homogenate was used to
705 inoculate HFF monolayers in Toxo medium. One to two weeks later, infected HFFs were

706 syringe-lysed and plated on new HFF monolayers to encourage parasite growth. Once
707 HFFs were fully vacuolated, parasites were passaged in Toxo medium supplemented with
708 mycophenolic acid (MPA) and xanthine that selects for parasites encoding a functional
709 *HXGPRT* (i.e. the challenging strains) and against the chronically infecting type III *hxgprt*-
710 which lacks a functional *HXGPRT* gene. Outgrowth in MPA-xanthine was considered
711 evidence for superinfection.

712 For counting tissue cysts, 100µl of brain homogenate was fixed in 900µL of ice
713 cold methanol, incubated for 5 minutes in microtubes (MCT-175-C, Axygen), washed and
714 stained overnight in a 500µL PBS solution containing 1:150 dilution of FITC-conjugated
715 *Dolichos biflorus* agglutinin (Vector Laboratories) with slow rotation at 4°C. The stained
716 homogenate was further washed and suspended in 1mL of PBS, of which several 50µL
717 aliquots were counted by fluorescence microscopy, and the number of cysts per brain
718 were deduced.

719 **Genetic linkage analysis**

720 Quantitative trait loci (QTL) analysis was performed with the package r/QTL in R (version
721 3.6.1). LOD scores for each marker were calculated using the Haley-Knott regression
722 model with the function 'scanone', or for all possible combination of two markers (i.e.
723 epistatic interactions) using the function 'scantwo'. 1000 permutations were performed to
724 obtain the genome wide LOD threshold for a P value of ≤0.05, which was considered
725 statistically significant. Similar results were obtained with a linear mixed regression model.
726 To estimate the effect each QTL had on the overall phenotype, the function 'fitqtl' was first
727 used to fit the data to a multiple-QTL model. Statistical support was found for inclusion of
728 all four QTLs with LOD scores > 3 compared to any lesser combination of three-QTLs
729 (ANOVA P <0.02). Individual QTL effects were then calculated under the assumption of

730 the four-QTL model, which collectively accounts for 91% of the observed phenotypic
731 variance.

732 **Cell isolation, in *vitro* recall infections, and FACS analysis**

733 PECs were isolated by peritoneal lavage and splenocytes obtained, as described in (Splitt
734 et al., 2018). In brief, 4mL of FACS buffer (PBS with 1% FBS) and 3mL of air were injected
735 into the peritoneal cavity with a 27G needle. After agitation, the PEC wash was poured
736 into a conical tube. PEC washes were filtered through a 70μm cell strainer, pelleted, and
737 washed with FACS buffer before staining. Spleens were dissected and crushed through
738 70μm cell strainers, pelleted, incubated in ACK red blood cell RBC lysis buffer (0.15M
739 NH_4Cl, 10mM $KHCO_3$, 0.1mM EDTA) for 5 minutes at room temperature, then washed
740 with FACS buffer. To obtain peripheral blood leukocytes (PBLs), 50μL of blood was
741 isolated from mice in tubes containing 5μL of 0.5 M EDTA on ice, pelleted and incubated
742 in ACK lysis buffer, washed and peripheral blood leukocytes (PBLs) were suspended in
743 FACS buffer.

744 For FACS analysis, all preparations were done on ice, and cells were blocked in
745 FACS buffer containing Fc Block anti-CD16/32 (2.4G2) (BD Biosciences), 5% normal
746 hamster serum, and 5% normal rat serum (Jackson ImmunoResearch) for 20 minutes
747 prior to staining with fluorophore-conjugated monoclonal antibodies (mAbs). The following
748 mAbs (1:100 staining dilutions) were used: anti-CD1d-BV650 (1B1, BD Bioscience), anti-
749 CD11c-eFlour 450 (N418, eBioscience); anti-CD11c-eFlour 450 (N418, BD Bioscience);
750 anti-CD45.2-eFlour 450 (104, eBioscience); anti-CD4-eFlour 450 (GK1.5, eBioscience),
751 anti-CD4-PECy7 (GK1.5, eBioscience); anti-CD11b-FITC (M1/70, eBioScience), anti-
752 CD11b-BUV395 (M1/70, BD Bioscience), anti-CD11b-BV421 (M1/70, BD Bioscience),
753 anti-CD11b-Pacific Blue (M1/70, BioLegend); anti-IFNγ-PE (XMG1.2, BD Bioscience);
754 anti-CD8α-APC (53-6.7, eBioscience), anti-CD8α-BV510 (53-6.7, BioLegend), anti-Ly6G-

755 APC (1A8-Ly6g, eBioscience), anti-CD19-PerCP-Cy5.5 (ebio1D3, eBioscience), anti-
756 CD19-PE (6D5, BioLegend), anti-CD19-BV785 (6D5, BioLegend), anti-CD3-eFlour 780
757 (17A2, BD Biosciences), anti-Ly6C-PECy7 (HK1.4, BioLegend), anti-CD23-Pacific Blue
758 (B3B4, BioLegend), anti-CD23-AF700 (B3B4, BioLegend), anti-CD21/CD35-FITC (7E9,
759 BioLegend), anti-CD21/CD35-PE (7E9, BioLegend), anti-CD5-APC (53-7.3, BioLegend),
760 anti-CD43-BV510 (S7, BD Bioscience), anti-CD43-BUV737 (S7, BD Bioscience), anti-
761 CD5-PerCP-Cy5.5 (53-7.3, BioLegend), anti-CD5- Cy7-APC (53-7.3, BioLegend), anti-
762 CD45R/B220-Cy7-APC (RA3-6B2, anti-CD45R/B220-BUV-661 (RA3-6B2, BD
763 Bioscience), anti-CD73-Cy7-PE (eBioTY/11.9, eBioscience), anti-CD80-BV711 (16-10A1,
764 BioLegend), anti-FCRL5-af88 (polyclonal, R&D systems) anti-IgM-PECy7 (RMM-1,
765 BioLegend), anti-IgM-BV605 (RMM-1, BioLegend), anti-IgD-FITC (11-26c.2a,
766 BioLegend), anti-IgD-PEDazzle (11-26c.2a, BioLegend), anti-CD138/Syndecan-1-BV510
767 (281-2, BD Bioscience), anti-CD138/Syndecan-1-BV650 (281-2, BioLegend), anti-mouse-
768 CD267/TACI-AlexaFlour-647 (8F10, BD Biosciences), and anti-CD268/BAFF-R-PE
769 (7H22-E16, BioLegend). Other FACS reagents included the viability dye propidium iodide
770 (Sigma) at a final concentration of 1µg/mL.

771 For *in vitro* recall, splenocytes and PerC were isolated from chronic and challenged
772 mice (day 5 or 7 following secondary infection) and 6 x 10^5 cells per well (96-well plate)
773 were plated in T cell medium (RPMI 1640 with GlutaMAX, 20% FBS, 1% Pen/Strep, 1mM
774 NaPyruvate, 10mM HEPES, 1.75µl BME). Cells were infected with a type I strain (RH or
775 GT1) strain at an MOI (multiplicity of infection) of 0.2 for 18 hr; 3µg/mL brefeldin A
776 (eBioscience) was added for the last 5 hr of infection. 96-well plates were placed on ice,
777 cells were harvested by pipetting and washed with FACS buffer, blocked, and stained for
778 surface markers. Cells were fixed with BD Cytofix/Cytoperm and permeabilized with BD
779 Perm/Wash solution (cat# 554714, BD Pharmingen), stained with anti-IFNγ-PE (XMG1.2,

780 BD Bioscience), anti-GZB (GB11, BioLegend) and anti-IL-2-APC (JES6-5H4, BioLegend)
781 on ice for 1 hr or overnight. Cells were then washed once with BD Perm/Wash solution,
782 once in FACS buffer, and analyzed by FACS.

783 For FoxP3 staining, peritoneal lavage was performed on chronic and challenged
784 (day 7 following secondary infection) bumble and WT mice. Cells were washed and
785 surface stained. Fixation and permeabilization was performed with the eBioscience
786 Foxp3/Transcription Factor Staining Buffer Set (cat # 00-5523-00) before intracellular
787 staining with anti-Foxp3-PE (MF-14, BioLegend) according to the manufacturer's
788 recommendations. Flow cytometry was performed on a Beckman Coulter Cytoflex LX,
789 LSR II (BD Biosciences), or the Bio-Rad ZE5 and analyzed with FlowJo™ software.

790 For intracellular staining of IgG H/L PerC and splenocytes were surface stained
791 with anti-CD43-BV510 (S7, BD Bioscience), anti-CD19-PE (6D5, BioLegend), anti-IgD-
792 FITC (11-26c.2a, Biolegend), anti-IgM-PE/Cy7 (RMM-1, BioLegend), anti-CD5-APC (53-
793 7.3, BioLegend), anti-CD45R/B220-Cy7-APC (RA3-6B2). Cells were then fixed with BD
794 Cytofix/Cytoperm and permeabilized with BD Perm/Wash solution (cat# 554714, BD
795 Pharmingen), stained with anti-IgG(H+L)-a350 (Polyclonal, Invitrogen) for 30 minutes.
796 Cells were then washed once with BD Perm/Wash solution, once in FACS buffer, and
797 analyzed by FACS.

798 **Analysis of isotype-specific antibody reactivity to *Toxoplasma gondii* by flow**
799 **cytometry**

800 For serum reactivity analysis, syringe-lysed GFP-expressing strains (RH1-1 and GT1-
801 GFP) were fixed in 3% formaldehyde for 20 minutes, washed twice in PBS, and plated in
802 96 well micro-titer plates at $4x10^5$ parasites/well. The parasites were then incubated with
803 serum from chronically infected mice, at serum concentrations ranging from 10^{-2} to 10^{-6}
804 diluted in FACS buffer, for 20 minutes at 37°C. Parasites were then washed with FACS

805 buffer and placed on ice for incubation with anti-isotype detection antibodies depending
806 on application: anti-IgG3-BV421 (R40-82, BD Bioscience), anti-IgM-PE/Cy7 (RMM-1,
807 BioLegend), anti-IgG1-FITC (RMG1-1, BioLegend), anti-IgG1-APC (RMG1-1,
808 BioLegend), anti-IgG2b-FITC (RMG2b-1, BioLegend), anti-IgG2b-PE (RMG2b-1,
809 BioLegend), anti-IgG2a-FITC (RMG2a-62, BioLegend), anti-IgG2a-PerCP/Cy5.5
810 (RMG2a-62, BioLegend), anti-IgM-a-PE (DS-1, BD Bioscience), Anti-IgM-b-PE (AF6-78,
811 BD Bioscience).

812 **Parasite neutralization assay**

813 Heat-inactivated serum was used to coat live parasites for 20 minutes at 37°C before
814 infecting $5x10^5$ mouse embryonic fibroblasts/well (MEFs) in 96 well plates. Immediately
815 following addition of parasite to MEF wells, plates were spun at 1200rpm for 3 minutes to
816 synchronize infection. 2 hrs after initiation of infection, cells were placed on ice and
817 harvested by scraping with pipette tips. Cells were washed twice in FACS buffer,
818 suspended in 1:1000 PI in FACS buffer, and then analyzed by flow cytometry.

819 **SDS-PAGE and immunoblotting for parasite lysate antigen**

820 To generate parasite lysate antigens *Toxoplasma gondii* was cultured in HFF and
821 expanded to approximately $2x10^8$ parasites. Parasites were syringe-lysed, washed with
822 sterile 1X PBS and the parasite pellet was lysed with (1mL) 0.1% TritonX-100 detergent
823 in 1X PBS. Solubilized parasites were centrifuged at 2,000 RCF for 20 minutes to remove
824 large debris. The supernatant was aliquoted and stored at -80°C. Parasite lysate was
825 reduced with β-mercaptoethanol (BME) and separated via SDS-PAGE in 4-20% Mini-
826 PROTEAN TGX pre-cast gels (cat # 4561096, Bio-Rad) before transfer to PVDF
827 membrane using a Trans-Blot Turbo Mini PVDF Transfer Pack (cat # 1704156, Bio-Rad)
828 via Bio-Rad Transblot Turbo (cat # 1704150, Bio-Rad). Membranes were blocked with
829 10% fortified bovine milk dissolved in Tris-Buffered Saline with 0.1% Tween (TBS-T 0.1%)

830 for 1-2 hrs at room temperature or overnight at 4°C. Blots were then probed with heat-
831 inactivated serum in block at either 1:1,000 dilution for serum IgM analysis or 1:5,000
832 dilution for serum IgG analysis overnight at 4°C. Membranes were washed with TBS-T
833 0.1% three times for 20 minutes per wash. Blots were then incubated for one hr at room
834 temperature with goat α-mouse horseradish peroxidase (HRP)-conjugated antibodies
835 (SouthernBiotec): anti-IgM secondary 1:1000 (cat# 1020-05) and total anti-IgG secondary
836 1:5000 (cat# 1030-05). Membranes were then washed with TBS-T 0.1% three times and
837 developed with Immobilon® Forte Western HRP Substrate (WBLUF0500). All blots were
838 imaged via chemiluminescence on a ChemiDoc Touch (cat# 12003153, Bio-Rad). Image
839 Lab 6.1 software (Bio-Rad) was used for analysis of bands and total lane signal. Western
840 blots comparing A/J to C57BL/6J were developed simultaneously and the band signal was
841 normalized to A/J.

842 **RNA isolation and sequencing**

843 Peritoneal B-1a (B220$^{int\text{-}neg}$ CD19^{high} CD11b+ CD5+ PI-), B-1b (B220$^{int\text{-}neg}$ CD19^{high}
844 CD11b+ CD5- PI-), or B-2 B cells (B220^{high} CD19+ CD11b- PI-) were sorted into 500ul
845 RNeasy lysis buffer using a FACS ARIA II cell sorter (BD Biosciences). RNA was purified
846 using the RNeasy mini kit (cat# 74134, Qiagen) according to the manufacturer's protocol.
847 RNA purity was tested by Qubit (ThermoFisher) and Agilent 2100 BioAnalyzer for total
848 RNA with picogram sensitivity. DNA libraries were generated with a Lexogen QuantSeq-
849 UMI FWD 3′ mRNA-Seq Library Prep Kit (cat# 015). Samples were sent to UC Davis for
850 QuantSeq 3' mRNA FWD-UMI sequencing.

851 **Gene expression analysis and data availability**

852 Raw reads were trimmed and mapped by the BlueBee genomic pipeline FWD-UMI Mouse
853 (GRCm38) Lexogen Quantseq 2.6.1 (Lexogen). In brief, reads were quality controlled with
854 'FASTQC', trimmed with 'Bbduk' to remove low quality tails, poly(A)read-through and

855 adapter contaminations, read alignments to the *Mus musculus* genome build GRCm38
856 were done with 'STAR', and gene reads were quantified with 'HTSeq-count'. Differentially
857 expressed gene (DEG) analysis was performed utilizing limma-voom in R version 3.6.3 in
858 RStudio with Bioconductor suite of packages. Heatmaps were generated with 'gplots'.
859 Pathway and GO term analysis was performed with MouseMine (mousemine.org), and
860 gene set enrichment analysis was performed with GSEA v4.0.3. RNA-sequencing data
861 generated in this study has been deposited in the NCBI Sequence Read Archive
862 (Bioproject accession number PRJNA637442). All other data that support the findings
863 herein are available from the corresponding author upon reasonable request.

864 **LPS-stimulation of enriched B cells and quantitative PCR**

865 PerC and splenocytes were isolated from naïve 6-8 week-old C57BL/6J and A/J mice and
866 enriched for B cells using the EasySep Mouse Pan B cell Isolation Kit (cat#19844,
867 StemTech). Bead enrichment for splenic samples had the addition of biotinylated anti-
868 CD43 antibodies (clone S7, BD Bioscience) to remove B-1 cells. Enriched samples were
869 plated in a 96-well plate at 400,000 cells per well and stimulated with 25ug/ml of LPS (cat#
870 L4391-1MG, Sigma). After 2 hrs, total RNA was isolated using the Rneasy Mini Kit (cat#
871 74134) and cDNA was synthesized using High Capacity cDNA Reverse Transcription Kit
872 (ThermoFisher, cat#4368814). Quantitative PCR was performed on synthesized cDNA
873 samples using ThermoFisher TaqMan Master Mix (cat# 4444556) and TaqMan probes:
874 *Actb* - Assay ID:Mm02619580_g1 (cat# 4331182), and *Nfkbid* - Assay ID:
875 Mm00549082_m1 (cat# 4331182), according to the manufacturer's protocol.
876 Normalization of *Nfkbid* expression in each sample was calculated in comparison to *Actb*
877 expression levels. Fold change in *Nfkbid* expression of AJ relative to that of C57BL/6J
878 cells was determined through the delta delta CT method ($2^{-\Delta\Delta CT}$).

879 **PerC adoptive transfers and IgH allotype chimeric mouse generation**

880 PerC was harvested by peritoneal lavage of 6-12 week old C57BL/6J donor mice as
881 described above and $5x10^6$ total peritoneal exudate cells (total PerC)/60ul PBS dose were
882 transferred i.p. into 2-4 day old bumble neonates. Allotype chimeric mouse generation was
883 performed as previously described (Lalor et al., 1989). In brief, 1-day old C57BL/6J
884 neonates were treated with 0.1mg of anti-IgM-b (clone AF6-78) and twice weekly
885 thereafter treated with 0.2mg of anti-IgM-b for 6 weeks. On day 2 after birth the neonates
886 were given $5x10^6$ total PerC from B6.Cg-*Gpi1*^{a} *Thy1*^{a} *Igh*^{a} delivered i.p. The mice were
887 then allowed to rest for 6 weeks after the last antibody treatment before infection with *T.*
888 *gondii*.

889 **Bone marrow chimeric mice generation**

890 B6.SJL-*Ptprc*^{a} *Pepc*^{b}/BoyJ, bumble, and C57BL/6J recipient mice were given 2 doses of
891 500cGy with an X-Rad320 (Precision X-Ray) with a 4 hr interval. Donor BM cells were
892 harvested from bumble and WT C57BL/6J mice, filtered with a 70um filter, incubated in
893 ACK red blood cell lysis buffer, washed with PBS and transplanted by retro-orbital injection
894 at a concentration of 10^7 cells/200ul PBS dose. For BM chimeras reconstituted with PerC,
895 $5*10^6$ total PerC from WT C57BL/6J mice were transferred I.P. Recipient mice were then
896 allowed to rest for 8 weeks. Reconstitution was assessed at 8 weeks by FACS analysis of
897 PBL.

898 **ELISA**

899 High-affinity protein binding microplates (Corning) were coated overnight goat anti-mouse
900 IgM (1mg/ml, Southern Biotech, cat# 1021-01) and blocked with coating buffer containing
901 with 1% BSA (w/v) and 2% goat serum (Omega Scientific) in PBS. Wells were washed
902 with ELISA wash buffer (1X PBS, 0.05% TweenTM-20). Mouse serum samples were
903 diluted 1:400 in coating buffer and incubated in the wells for 1 hr. Wells were washed 5
904 times and secondary goat anti-IgM-HRP (Southern Biotech, cat# 1021-08) at 1:5000

905 dilution was incubated for 1 hr in the wells. Wells were washed several times and
906 developed with TMB substrate (Invitrogen). Development was stopped after 20 minutes
907 with 1M H_3PO_4 stop solution. Absorbance was measured at 450nm on a BioTek Epoch
908 microplate spectrophotometer.

909 **Statistics**

910 Statistical analysis was performed with Graphpad Prism 8 software. Statistical significance
911 was defined as $P < 0.05$. P values were calculated using paired or unpaired two-tailed t-
912 tests, 2-way ANOVA with Tukey multiple comparison correction, and multiple t-tests with
913 the Holm-Sidak correction for multiple comparisons. Survival curve significance was
914 calculated using log-rank (Mantel-Cox) testing. Significance in time to death was
915 calculated using the Gehan-Breslow-Wilcoxon test. Differential gene expression analysis
916 statistics were calculated using the Limma-Voom R package, P values were adjusted with
917 the Benjamini-Hochberg correction for multiple comparisons. GO term and pathway
918 enrichment analysis statistics were performed at mousemine.org using the Holm-
919 Bonferroni test correction. Statistical methods used for each figure are indicated in the
920 figure legends.

921

922 **SUPPLEMENTAL INFORMATION**

923

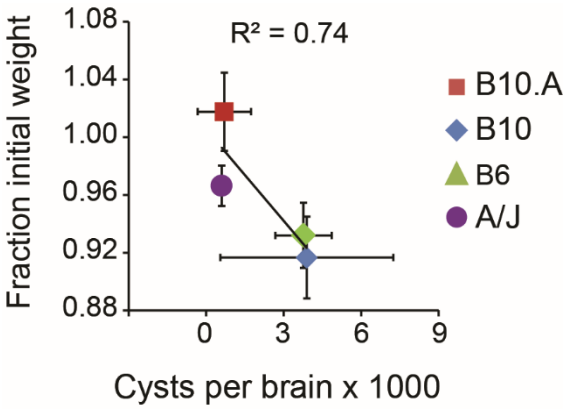

924

925

926 **Figure S1. Cyst burden and weight during chronic infection with the low virulent**

927 **type III CEP strain correlates with the murine H-2 locus.**

928 A/J, C57BL/6J (B6), C57BL/10J (B10), and C57BL/10.AJ (B10.A) mice were injected with

929 the type III strain *CEP hxgprt*- and allowed to progress to chronic infection. Plotted (+/-

930 SEM) is the average cyst number (x 1000) in the brain vs. the average fraction of initial

931 weight, where 1 is the normalized weight on the day of type III injection; the regression

932 value (R^2) is indicated. Results are from 3 to 5 mice for cyst numbers (day 42 of chronic

933 infection), and 5-12 mice for weight measurements (day 30 of chronic infection) per mouse

934 strain.

935

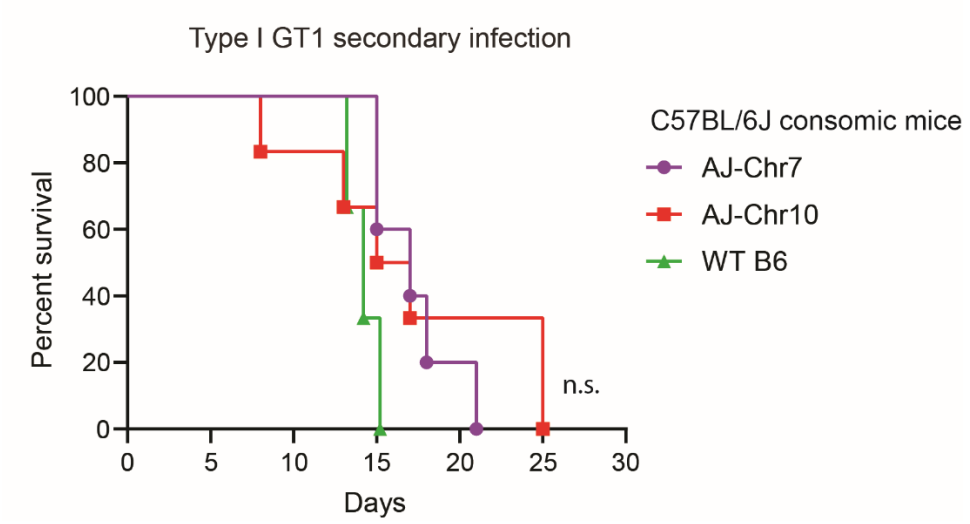

936

937 **Figure S2. Consomic mice succumb to type I GT1 secondary infection.**

938 Consomic mice of the C57BL/6J background with A/J chromosomal substitutions for

939 chromosome 7 (C57BL/6J-Chr7$^{A/J}$/NaJ) or chromosome 10 (C57BL/6J-Chr10$^{A/J}$/NaJ)

940 were infected with the type III CEP *hxgprt*- strain and allowed to progress to chronic

941 infection. Mice were then given a secondary infection with the type I GT1 strain.

942 Cumulative survival is shown for 2 independent experiments (CSS7 n=5, CSS10 n=6);

943 n.s., Mantel-Cox.

944

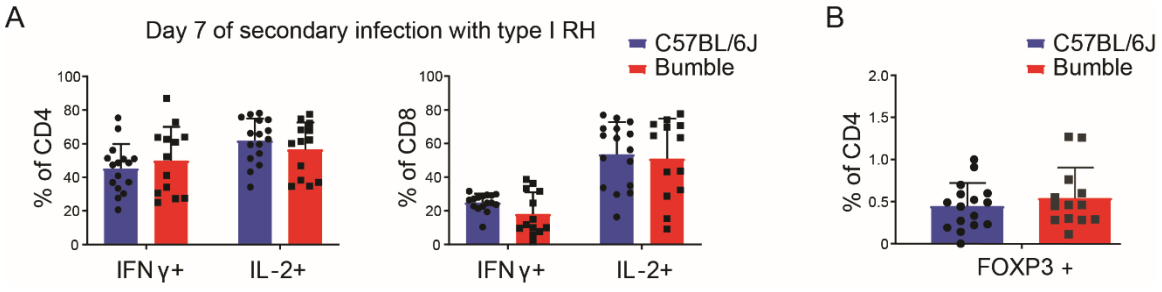

Figure S3. Bumble mice have intact T cell responses during secondary infection. A) Peritoneal CD4 and CD8 T cells from bumble and C57BL/6J mice were assessed at day 7 of secondary infection with the type I RH strain by an in vitro recall assay and assayed for intracellular IFNγ and IL-2. In brief, peritoneal cells were harvested and infected with live type I RH parasites for 16 hrs. T cells were assessed for production of granzyme IFNγ, and IL-2 by intracellular staining and FACS. B) Peritoneal T-regulatory cells (CD4+ CD25+ Foxp3+) were quantified at day 7 of secondary infection with type I RH strain. Each dot represents the result from one mouse, and plotted are cumulative averages +SD from 3 experiments; no significant differences were observed between bumble and C57BL/6J mice by unpaired t-tests with the Holm-Sidak correction for multiple comparisons.

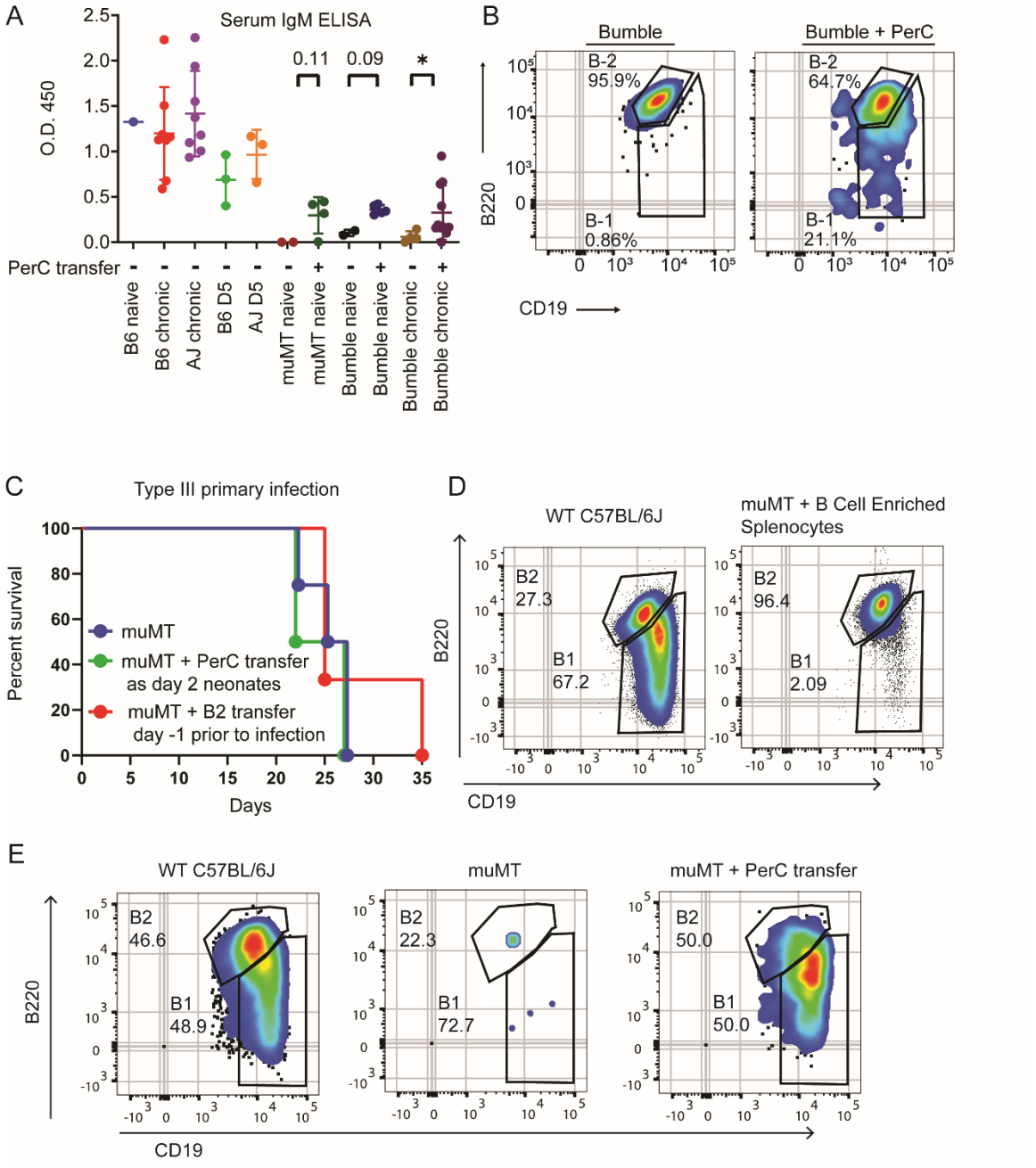

Figure S4. Assessing PerC reconstitutions by serum IgM ELISAs and flow cytometry, and survival of muMT mice.

A) Serum IgM from C57BL/6J, muMT, bumble, and A/J mice was measured by ELISA. Serum was harvested from mice either naïve, chronically infected with type III CEP strain, or on D5 post-secondary infection with type I GT1 *T. gondii* strain. PerC transfer (+) refers

964 to mice adoptively transferred $5x10^6$ total PerC cells as a day 2 neonate. Each dot
965 represents the results from an individual mouse, and plotted is the average +/-SD of the
966 O.D. obtained at 450nm; *P<0.05, unpaired two-tailed t-test. B) Bumble reconstitution of
967 the peritoneal B-1 compartment after neonatal PerC adoptive transfer. Representative
968 FACS plots of peritoneal B-2 cells ($B220^{high}$ CD19+) and B-1 ($B220^{int\text{-}neg}$ CD19+) cells from
969 bumble mice with or without PerC adoptive transfer. Shown are mice on day 20 of primary
970 infection with the type III CEP strain. C) B cell deficient muMT mice (n=3), muMT given
971 WT PerC adoptive transfers as 2-day neonates then allowed to reconstitute for 6-7 weeks
972 into adulthood (n=2), and muMT given B cell enriched splenocytes (n=3) 1 day prior to
973 infection with the type III CEP strain were assessed for survival. D) muMT reconstitution
974 of B-2 cell compartment, WT and muMT with B cell enriched splenocytes (EasySep™
975 Mouse Pan-B Cell Isolation Kit, cat# 19844) adoptively transferred 24 hrs earlier E) muMT
976 reconstitution of peritoneal B cell compartment after neonatal adoptive transfer.
977 Representative FACS plots of peritoneal B-2 cells (B220high CD19+) and B-1 B cells
978 (B220int-neg CD19+) from WT, and muMT mice or muMT mice with neonatal PerC
979 adoptive transfer. For D and E, uninfected mice are 6-8 weeks of age and numbers
980 indicate the percent of cells that fall within the depicted gate.
981

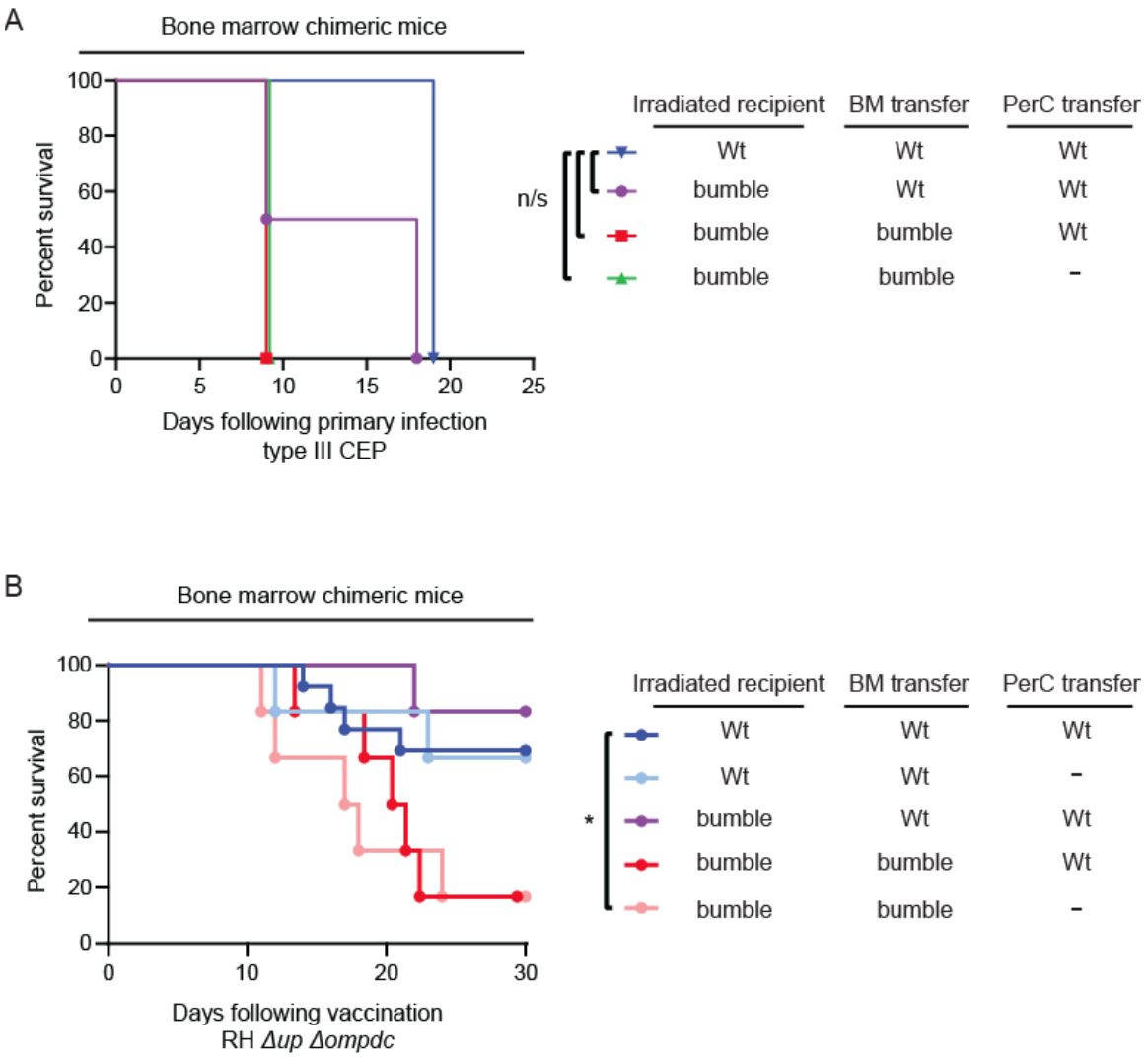

Figure S5. Bone marrow chimeric mice fail to survive primary infection but exhibit improved survival to vaccine strains.

A) Survival of the indicated bone marrow (BM) chimeras infected with the type III CEP *T. gondii* strain are plotted from a single experiment (n=2 for bumble recipients per condition; n=1 for C57BL/6J recipients); n.s., Mantel-Cox. B) Survival of the indicated BM chimeras vaccinated (10^6 i.p.) with the uracil auxotroph strain, Rh *Δup Δompdc*. Results are cumulative from 2-3 separate transfers and vaccinations; (n=4-9 per condition).

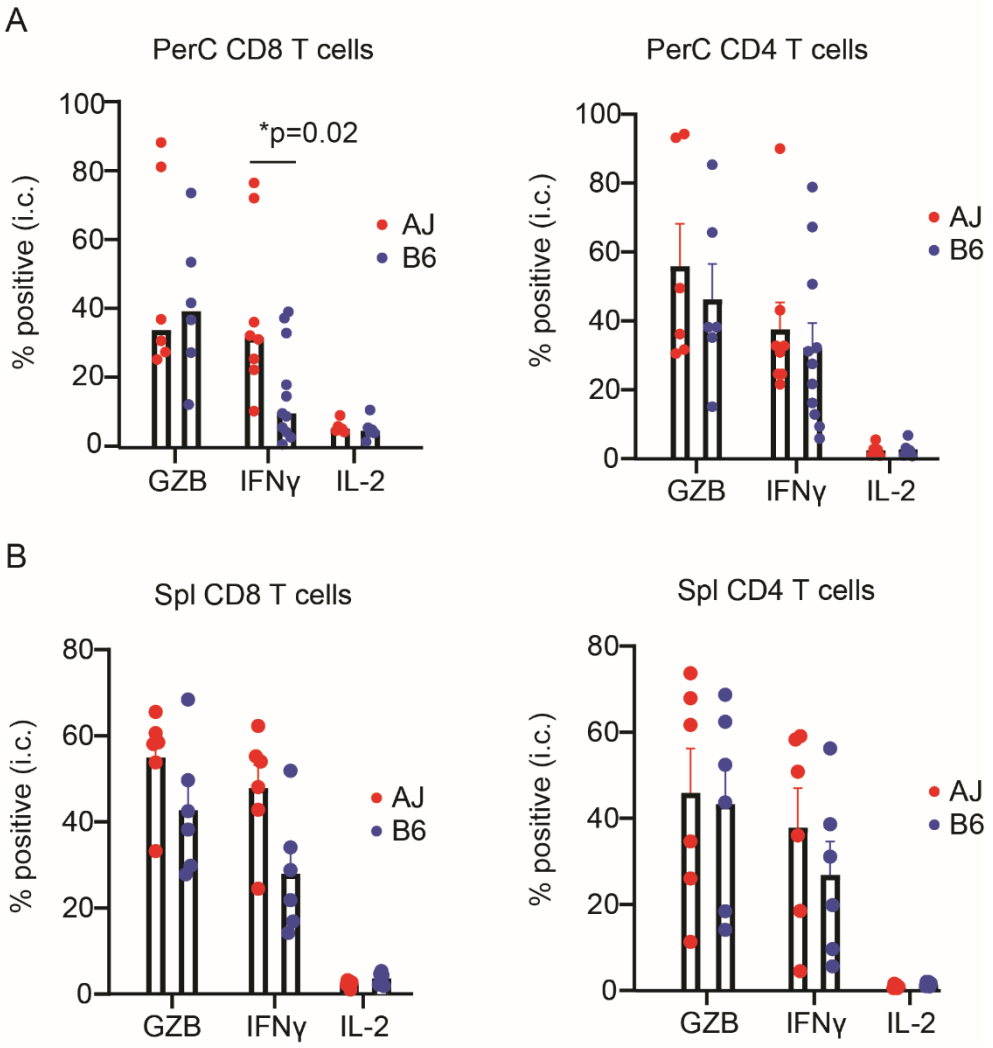

991

992 **Figure S6. CD8 T cell IFNγ frequencies are increased in resistant A/J mice.**

993 A) Peritoneal and B) splenic cells were harvested from A/J and C57BL6/J mice chronically

994 infected with type III CEP *T. gondii* strain, and infected with live type I parasites for 16 hrs.

995 T cells were assessed for production of granzyme B (GZB), IFNγ, and IL-2 by intracellular

996 staining and FACS. The average frequency +/-SD of positive staining CD4+ or CD8+ T

997 cells (CD3+ CD19-) and cumulative results from 2-3 experiments (AJ n=8, C57BL6/J

998 n=11) are shown; * P<0.05, unpaired two-tailed t-test.

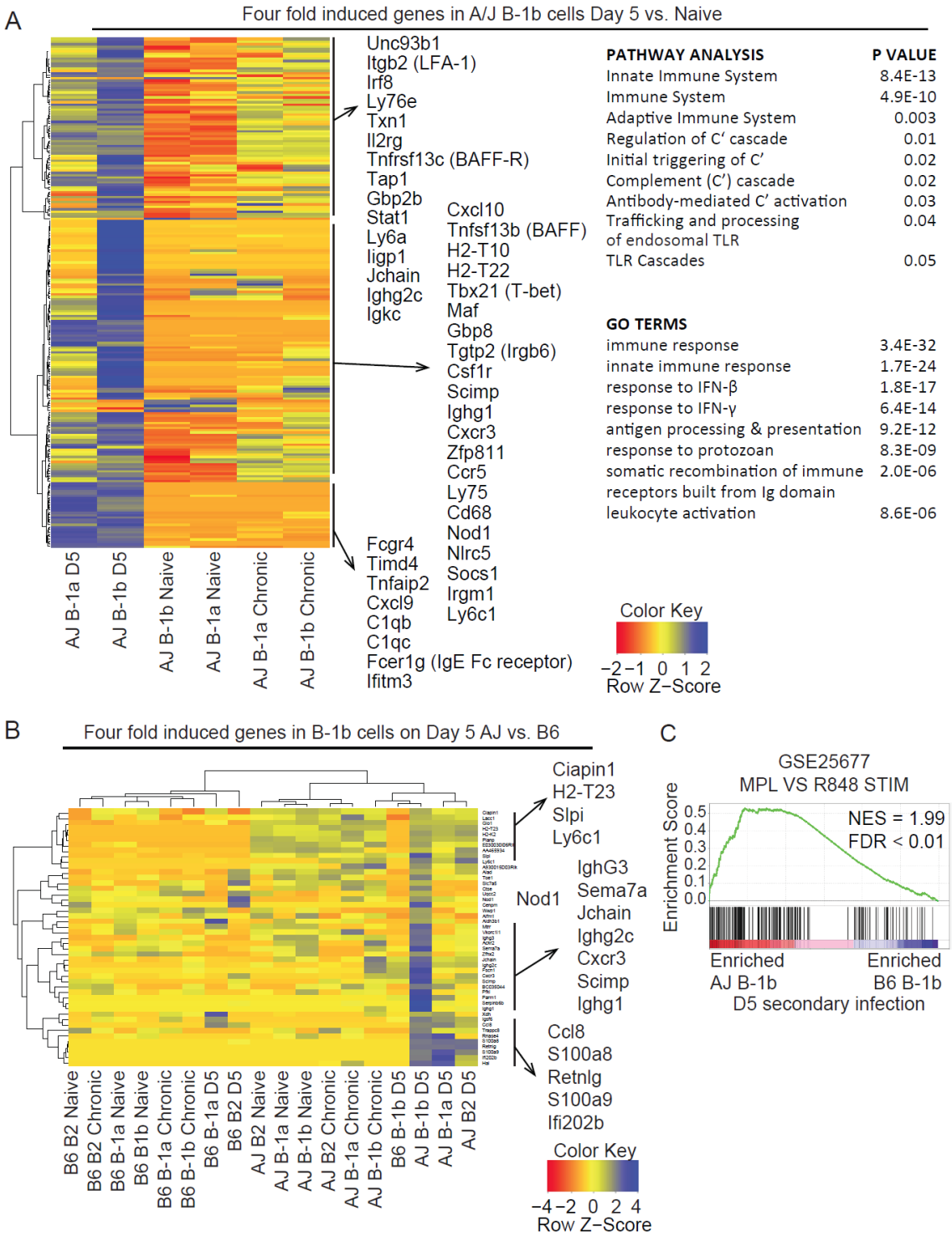
A
Four fold induced genes in A/J B-1b cells Day 5 vs. Naive
Unc93b1
Itgb2 (LFA-1)
Irf8
Ly76e
Txn1
Il2rg
Tnfrsf13c (BAFF-R)
Tap1
Gbp2b
Stat1
Ly6a
Iigp1
Jchain
Ighg2c
Igkc
Cxcl10
Tnfsf13b (BAFF)
H2-T10
H2-T22
Tbx21 (T-bet)
Maf
Gbp8
Tgtp2 (Irgb6)
Csf1r
Scimp
Ighg1
Cxcr3
Zfp811
Ccr5
Ly75
Cd68
Nod1
Nlrc5
Socs1
Irgm1
Ly6c1
Fcgr4
Timd4
Tnfaip2
Cxcl9
C1qb
C1qc
Fcer1g (IgE Fc receptor)
Ifitm3
AJ B-1a D5
AJ B-1b D5
AJ B-1b Naive
AJ B-1a Naive
AJ B-1a Chronic
AJ B-1b Chronic
PATHWAY ANALYSIS
P VALUE
Innate Immune System 8.4E-13
Immune System 4.9E-10
Adaptive Immune System 0.003
Regulation of C' cascade 0.01
Initial triggering of C' 0.02
Complement (C') cascade 0.02
Antibody-mediated C' activation 0.03
Trafficking and processing of endosomal TLR 0.04
TLR Cascades 0.05
GO TERMS
immune response 3.4E-32
innate immune response 1.7E-24
response to IFN-β 1.8E-17
response to IFN-γ 6.4E-14
antigen processing & presentation 9.2E-12
response to protozoan 8.3E-09
somatic recombination of immune receptors built from Ig domain 2.0E-06
leukocyte activation 8.6E-06
Color Key
−2 −1 0 1 2
Row Z−Score
B
Four fold induced genes in B-1b cells on Day 5 AJ vs. B6
Ciapin1
H2-T23
Slpi
Ly6c1
IghG3
Sema7a
Nod1
Jchain
Ighg2c
Cxcr3
Scimp
Ighg1
Ccl8
S100a8
Retnlg
S100a9
Ifi202b
B6 B2 Naive
B6 B2 Chronic
B6 B-1a Naive
B6 B1b Naive
B6 B-1a Chronic
B6 B-1b Chronic
B6 B-1a D5
B6 B2 D5
AJ B2 Naive
AJ B-1a Naive
AJ B-1b Naive
AJ B2 Chronic
AJ B-1a Chronic
AJ B-1b Chronic
B6 B-1b D5
AJ B-1b D5
AJ B-1a D5
AJ B2 D5
Color Key
−4 −2 0 2 4
Row Z−Score
C
GSE25677
MPL VS R848 STIM
Enrichment Score
0.5
0.4
0.3
0.2
0.1
0.0
NES = 1.99
FDR < 0.01
Enriched
AJ B-1b
Enriched
B6 B-1b
D5 secondary infection

1002 **Figure S7. Genes uniquely induced in B-1b cells on day 5 of secondary infection in**
1003 **resistant A/J mice.**
1004 Transcriptomic analysis of peritoneal B-1a (CD19+ B220$^{int-neg}$ CD11b+ CD5+), B-1b
1005 (CD19+ B220$^{int-neg}$ CD11b+ CD5-) and B-2 (CD19+ B220^{hi} CD11b- CD5-) B cells from A/J
1006 and C57BL/6J mice was performed using 3'-Tag RNA sequencing. A) Genes that were
1007 differentially upregulated in B-1b cells on day 5 of secondary infection compared to naïve
1008 mice in the A/J genetic background. P values of differentially expressed genes were
1009 calculated using the Benjamini-Hochberg adjustment for false discovery rate, and only
1010 those genes that survived significance were included in the heatmap. For comparison, all
1011 B-1 compartments in A/J mice are shown for this gene set. A/J B-1 Pathway and GO term
1012 enrichment was assessed on the genes presented in the heatmap in A. P values for
1013 enrichment analysis were adjusted with the Holm-Bonferroni correction. B) A cluster of
1014 genes found to be differentially induced in B-1b cells in A/J compared to C57BL/6J mice
1015 on day 5 of secondary infection are plotted as a heat map. C) Gene set enrichment
1016 analysis of the rank-ordered list of differentially expressed genes between A/J and
1017 C57BL/6J B-1b cells at D5 of secondary infection. Gene set depicted was in the top 10
1018 gene sets ranked by false discovery rate (FDR) after investigating MSigDB's C7:
1019 immunologic signatures collection. Enrichment score is the degree of overrepresentation
1020 of a gene set at the top or bottom of a ranked list. NES is the enrichment score after
1021 normalizing for gene set size.

Mouse Strain	Chronic Infection	Secondary Infection	[1]Heterologous Brain Coinfection?
C57BL/10	CEP *hxgprt-*	GUYMAT	1/1
Cumulative average C57BL/10			1/1 = 100%
C57BL/10.A	CEP *hxgprt-*	TgCATBr5	2/2
C57BL/10.A	CEP *hxgprt-*	GUYMAT	2/2
C57BL/10.A	CEP *hxgprt-*	MAS	1/2
C57BL/10.A	CEP *hxgprt-*	FOU	0/1
Cumulative average C57BL/10.A			5/7 = 71%
A/J	CEP *hxgprt-*	GUYMAT	0/4
A/J	CEP *hxgprt-*	TgCATBr5	0/5
A/J	CEP *hxgprt-*	GUYDOS	4/5
A/J	CEP *hxgprt-*	VAND	4/6
A/J	CEP *hxgprt-*	FOU	1/5
A/J	CEP *hxgprt-*	GPHT	0/5
A/J	CEP *hxgprt-*	MAS	0/5
Cumulative average A/J			9/35 = 26%

1022

1023 **Table S1. Virulent strains of *Toxoplasma gondii* superinfect genetically resistant**
1024 **hosts.**

1025 CEP *hxgprt-* chronically infected C57BL/10, C57BL/10.A, and A/J mice were given a
1026 secondary infection with the indicated atypical *T. gondii* strain; then, 35-45 days after
1027 secondary infection, brains from surviving mice were homogenized in PBS and used to
1028 inoculate HFF monolayers. The resultant parasite cultures were then tested for the
1029 presence of the secondary infection strain; numerator = number of mice tested positive for
1030 secondary infection strain in the brain; denominator = number of mice that exhibited
1031 parasite growth in the HFF monolayer prior to drug selection.

1032 [1]Parasite growth was observed in mycophenolic acid / xanthine medium, which selects for

1033 parasites encoding a functional *HXGPRT* gene (i.e. the challenging atypical strains) and

1034 kills the primary infection CEP *hxgprt-* strain.

1035
1036

Recombinant Inbred Strain	Type III CEP Primary Infection Survival	Type I GT1 Secondary Infection Survival	[1]Heterologous Brain Coinfection?
AXB1	100	0	N/A
AXB2	100	100	0/2
AXB4	0	N/A	N/A
AXB5	50	100	1/1
AXB6	0	N/A	N/A
AXB8	100	50	1/1
AXB10	0	N/A	N/A
AXB12	100	100	2/2
AXB13	0	N/A	N/A
AXB15	100	100	1/2
AXB19	100	0	N/A
AXB23	100	0	N/A
AXB24	100	0	N/A
BXA1	50	0	N/A
BXA2	100	0	N/A
BXA4	100	100	0/1
BXA7	100	0	N/A
BXA8	100	100	2/2
BXA11	100	0	N/A
BXA12	100	100	1/1
BXA13	100	100	0/1
BXA14	100	0	N/A
BXA16	100	0	N/A
BXA24	100	50	N/A
BXA25	100	100	1/2
BXA26	100	100	0/2
Cumulative Average	82.6%	50%	9/17 = 52.9%

1037

1038

1039 **Table S2. Primary and secondary infection survival of recombinant inbred mice**
1040 **(AxB;BxA).**

1041 26 strains (n = 2) from the RI (AxB; BxA) panel were infected with 10^4 type III avirulent
1042 CEP *hxgprt- T. gondii* parasites; then, 35 days later, mice were challenged with $5x10^4$
1043 virulent type I GT1 *T. gondii* parasites. Primary and secondary infection survival
1044 percentages are indicated. 35-45 days after secondary challenge, brains from the
1045 surviving RI mice were homogenized in PBS and used to inoculate HFF monolayers. The
1046 resultant parasite cultures were then tested for the presence of the challenging strain;
1047 numerator = number of mice tested positive for secondary infection strain in the brain;
1048 denominator = number of mice that exhibited parasite growth in the HFF monolayer prior
1049 to drug selection. Some surviving mice failed to generate parasite positive cultures.

1050 [1]Parasite growth was observed in mycophenolic acid / xanthine medium, which selects for
1051 GT1 parasites (the challenging strain) encoding the endogenous *HXGPRT* gene and
1052 against the primary infection CEP *hxgprt-* strain.

1053

1054

1055 **Dataset S1. Polymorphic genes between A/J and C57BL/6J encoded within the four**
1056 **QTLs that define immunity to *Toxoplasma gondii.***
1057 For each of the four QTLs that define secondary infection immunity to *T. gondii*, a list of
1058 all genes that have a DNA polymorphism between A/J and C5BL/6J mice, and are
1059 encoded within the QTL boundaries defined by the maximal genetic marker (real or
1060 imputed markers inferred in r/QTL) and the two flanking markers on either side; LOD
1061 scores and position are indicated. For each gene, its location and unique identifiers are
1062 listed, as well as the number and class of small nucleotide polymorphism (SNP) between
1063 A/J and C57BL/6J are shown. Total number of SNPs for each gene were also tallied ('Sum
1064 mutation'), and in bold are genes who's SNPs are two standard deviations greater than
1065 the average SNP for that class within the QTL region. In these QTL regions, there were
1066 also 476 (chr7), 88 (chr10), 40 (chr11) and 375 SNPs (chr17) that did not associate with
1067 any gene in the QTL boundaries. UTR, untranslated region; 'Region SNP', SNPs that are
1068 +/- 2 kb of the gene boundaries. Data obtained from Mouse Genome Informatics (MGI)
1069 (informatics.jax.org), and each locus is in a separate tab.
1070
1071 **Dataset S2. Transcriptomic analysis of B cells responding to *Toxoplasma gondii***
1072 **infection.**
1073 Table of genes included (threshold of >=5 CPM in any sample) in differential gene
1074 expression analysis. For each gene the Ensembl ID, MGI ID, gene symbol and
1075 descriptions are listed. The CPM from 3 samples of peritoneal B-1a, B-1b, and B-2 at
1076 naïve (N), chronic (Ch), and day 5 (D5) of secondary infection in both A/J (AJ) and
1077 C57BL/6J (B6) mice are given. The average CPM was calculated for each set of samples
1078 and average counts less than 5 CPM were raised to 5 to reduce the effect of low
1079 expression genes in further analysis. The log2 fold change (FC) of gene expression was

1080 calculated using the average CPM for each cell type (B-1a, B-1b, and B-2) of each strain
1081 (A/J and C57BL/6J) as they progressed from naïve to chronic infection or chronic to D5
1082 secondary infection. The Log2 FC was also calculated from naïve to D5 of secondary
1083 infection. The Log2 FC between A/J and C57BL/6J was calculated for each cell type.
1084 Genes were then ranked by the number of comparisons that exhibited greater than 4FC
1085 by the indicated comparison.

1086

1087 **REFERENCES**

1088

1089 Alugupalli, K.R., Leong, J.M., Woodland, R.T., Muramatsu, M., Honjo, T., and Gerstein,
1090 R.M. (2004). B1b lymphocytes confer T cell-independent long-lasting immunity.
1091 Immunity *21,* 379-390.

1092 Arnold, C.N., Pirie, E., Dosenovic, P., McInerney, G.M., Xia, Y., Wang, N., Li, X., Siggs,
1093 O.M., Karlsson Hedestam, G.B., and Beutler, B. (2012). A forward genetic screen
1094 reveals roles for Nfkbid, Zeb1, and Ruvbl2 in humoral immunity. Proc. Natl. Acad. Sci. U.
1095 S. A. *109,* 12286-12293.

1096 Baumgarth, N., Jager, G.C., Herman, O.C., and Herzenberg, L.A. (2000). CD4+ T cells
1097 derived from B cell-deficient mice inhibit the establishment of peripheral B cell pools.
1098 Proc. Natl. Acad. Sci. U. S. A. *97,* 4766-4771.

1099 Berthier-Vergnes, O., El Kharbili, M., de la Fouchardiere, A., Pointecouteau, T.,
1100 Verrando, P., Wierinckx, A., Lachuer, J., Le Naour, F., and Lamartine, J. (2011). Gene
1101 expression profiles of human melanoma cells with different invasive potential reveal
1102 TSPAN8 as a novel mediator of invasion. Br. J. Cancer *104,* 155-165.

1103 Blandino, R., and Baumgarth, N. (2019). Secreted IgM: New tricks for an old molecule.
1104 J. Leukoc. Biol. *106,* 1021-1034.

1105 Brown, C.R., Hunter, C.A., Estes, R.G., Beckmann, E., Forman, J., David, C.,
1106 Remington, J.S., and McLeod, R. (1995). Definitive identification of a gene that confers
1107 resistance against Toxoplasma cyst burden and encephalitis. Immunology *85,* 419-428.

1108 Casciotti, L., Ely, K.H., Williams, M.E., and Khan, I.A. (2002). CD8(+)-T-cell immunity
1109 against Toxoplasma gondii can be induced but not maintained in mice lacking
1110 conventional CD4(+) T cells. Infect. Immun. *70,* 434-443.

1111 Castigli, E., Wilson, S.A., Scott, S., Dedeoglu, F., Xu, S., Lam, K.P., Bram, R.J., Jabara,
1112 H., and Geha, R.S. (2005). TACI and BAFF-R mediate isotype switching in B cells. J.
1113 Exp. Med. *201,* 35-39.

1114 Chen, M., Mun, H.S., Piao, L.X., Aosai, F., Norose, K., Mohamed, R.M., Belal, U.S.,
1115 Fang, H., Ahmed, A.K., Kang, H.K.*, et al.* (2003). Induction of protective immunity by

1116 primed B-1 cells in Toxoplasma gondii -infected B cell-deficient mice. Microbiol.
1117 Immunol. *47,* 997-1003.

1118 Choi, Y.S., and Baumgarth, N. (2008). Dual role for B-1a cells in immunity to influenza
1119 virus infection. J. Exp. Med. *205,* 3053-3064.

1120 Couper, K.N., Roberts, C.W., Brombacher, F., Alexander, J., and Johnson, L.L. (2005).
1121 Toxoplasma gondii-specific immunoglobulin M limits parasite dissemination by
1122 preventing host cell invasion. Infect. Immun. *73,* 8060-8068.

1123 Fox, B.A., and Bzik, D.J. (2010). Avirulent uracil auxotrophs based on disruption of
1124 orotidine-5'-monophosphate decarboxylase elicit protective immunity to Toxoplasma
1125 gondii. Infect. Immun. *78,* 3744-3752.

1126 Gazzinelli, R.T., Hakim, F.T., Hieny, S., Shearer, G.M., and Sher, A. (1991). Synergistic
1127 role of CD4+ and CD8+ T lymphocytes in IFN-gamma production and protective
1128 immunity induced by an attenuated Toxoplasma gondii vaccine. J. Immunol. *146,* 286-
1129 292.

1130 Gigley, J.P., Fox, B.A., and Bzik, D.J. (2009). Cell-mediated immunity to Toxoplasma
1131 gondii develops primarily by local Th1 host immune responses in the absence of
1132 parasite replication. J. Immunol. *182,* 1069-1078.

1133 Glatman Zaretsky, A., Silver, J.S., Siwicki, M., Durham, A., Ware, C.F., and Hunter, C.A.
1134 (2012). Infection with Toxoplasma gondii alters lymphotoxin expression associated with
1135 changes in splenic architecture. Infect. Immun. *80,* 3602-3610.

1136 Grigg, M.E., Ganatra, J., Boothroyd, J.C., and Margolis, T.P. (2001). Unusual
1137 Abundance of Atypical Strains Associated with Human Ocular Toxoplasmosis. J. Infect.
1138 Dis. *184,* 633 639.

1139 Ha, S.A., Tsuji, M., Suzuki, K., Meek, B., Yasuda, N., Kaisho, T., and Fagarasan, S.
1140 (2006). Regulation of B1 cell migration by signals through Toll-like receptors. J. Exp.
1141 Med. *203,* 2541-2550.

1142 Hassan, M.A., Jensen, K.D., Butty, V., Hu, K., Boedec, E., Prins, P., and Saeij, J.P.
1143 (2015). Transcriptional and Linkage Analyses Identify Loci that Mediate the Differential
1144 Macrophage Response to Inflammatory Stimuli and Infection. PLoS Genet. *11,*
1145 e1005619.

1146 Hoffman, S.L., Goh, L.M., Luke, T.C., Schneider, I., Le, T.P., Doolan, D.L., Sacci, J., de
1147 la Vega, P., Dowler, M., Paul, C.*, et al.* (2002). Protection of humans against malaria by
1148 immunization with radiation-attenuated Plasmodium falciparum sporozoites. J. Infect.
1149 Dis. *185,* 1155-1164.

1150 Hosokawa, J., Suzuki, K., Meguro, K., Tanaka, S., Maezawa, Y., Suto, A., Fujimura, L.,
1151 Sakamoto, A., Clevers, H., Ohara, O., and Nakajima, H. (2017). IkappaBNS enhances
1152 follicular helper T-cell differentiation and function downstream of ASCl2. J. Allergy Clin.
1153 Immunol. *140,* 288-291.e8.

1154 Howe, D.K., and Sibley, L.D. (1995). Toxoplasma gondii comprises three clonal
1155 lineages: correlation of parasite genotype with human disease. J. Infect. Dis. *172,* 1561-
1156 1566.

1157 Itakura, A., Szczepanik, M., Campos, R.A., Paliwal, V., Majewska, M., Matsuda, H.,
1158 Takatsu, K., and Askenase, P.W. (2005). An hour after immunization peritoneal B-1 cells

1159 are activated to migrate to lymphoid organs where within 1 day they produce IgM
1160 antibodies that initiate elicitation of contact sensitivity. J. Immunol. *175,* 7170-7178.

1161 Jensen, K.D., Camejo, A., Melo, M.B., Cordeiro, C., Julien, L., Grotenbreg, G.M., Frickel,
1162 E.M., Ploegh, H.L., Young, L., and Saeij, J.P. (2015). Toxoplasma gondii superinfection
1163 and virulence during secondary infection correlate with the exact ROP5/ROP18 allelic
1164 combination. MBio *6,* 2280.

1165 Johnson, L.L., and Sayles, P.C. (2002). Deficient humoral responses underlie
1166 susceptibility to Toxoplasma gondii in CD4-deficient mice. Infect. Immun. *70,* 185-191.

1167 Joiner, K.A., Fuhrman, S.A., Miettinen, H.M., Kasper, L.H., and Mellman, I. (1990).
1168 Toxoplasma gondii: fusion competence of parasitophorous vacuoles in Fc receptor-
1169 transfected fibroblasts. Science *249,* 641-646.

1170 Kang, H., Remington, J.S., and Suzuki, Y. (2000). Decreased resistance of B cell-
1171 deficient mice to infection with Toxoplasma gondii despite unimpaired expression of IFN-
1172 gamma, TNF-alpha, and inducible nitric oxide synthase. J. Immunol. *164,* 2629-2634.

1173 Kantor, A.B., Stall, A.M., Adams, S., Herzenberg, L.A., and Herzenberg, L.A. (1992).
1174 Differential development of progenitor activity for three B-cell lineages. Proc. Natl. Acad.
1175 Sci. U. S. A. *89,* 3320-3324.

1176 Khan, A., Jordan, C., Muccioli, C., Vallochi, A.L., Rizzo, L.V., Belfort, R.,Jr, Vitor, R.W.,
1177 Silveira, C., and Sibley, L.D. (2006). Genetic divergence of Toxoplasma gondii strains
1178 associated with ocular toxoplasmosis, Brazil. Emerg. Infect. Dis. *12,* 942-949.

1179 Khoenkhoen, S., Erikson, E., Adori, M., Stark, J.M., Scholz, J.L., Cancro, M.P.,
1180 Pedersen, G.K., and Karlsson Hedestam, G.B. (2019). TACI expression and plasma cell
1181 differentiation are impaired in the absence of functional IkappaBNS. Immunol. Cell Biol.
1182 *97,* 485-497.

1183 Kim, C.C., Baccarella, A.M., Bayat, A., Pepper, M., and Fontana, M.F. (2019). FCRL5(+)
1184 Memory B Cells Exhibit Robust Recall Responses. Cell. Rep. *27,* 1446-1460.e4.

1185 Kreuk, L.S., Koch, M.A., Slayden, L.C., Lind, N.A., Chu, S., Savage, H.P., Kantor, A.B.,
1186 Baumgarth, N., and Barton, G.M. (2019). B cell receptor and Toll-like receptor signaling
1187 coordinate to control distinct B-1 responses to both self and the microbiota. Elife *8,*
1188 10.7554/eLife.47015.

1189 Krishnamurty, A.T., Thouvenel, C.D., Portugal, S., Keitany, G.J., Kim, K.S., Holder, A.,
1190 Crompton, P.D., Rawlings, D.J., and Pepper, M. (2016). Somatically Hypermutated
1191 Plasmodium-Specific IgM(+) Memory B Cells Are Rapid, Plastic, Early Responders upon
1192 Malaria Rechallenge. Immunity *45,* 402-414.

1193 Kuwata, H., Matsumoto, M., Atarashi, K., Morishita, H., Hirotani, T., Koga, R., and
1194 Takeda, K. (2006). IkappaBNS inhibits induction of a subset of Toll-like receptor-
1195 dependent genes and limits inflammation. Immunity *24,* 41-51.

1196 Lalor, P.A., Herzenberg, L.A., Adams, S., and Stall, A.M. (1989). Feedback regulation of
1197 murine Ly-1 B cell development. Eur. J. Immunol. *19,* 507-513.

1198 Lorenzi, H., Khan, A., Behnke, M.S., Namasivayam, S., Swapna, L.S., Hadjithomas, M.,
1199 Karamycheva, S., Pinney, D., Brunk, B.P., Ajioka, J.W., *et al.* (2016). Local admixture of
1200 amplified and diversified secreted pathogenesis determinants shapes mosaic
1201 Toxoplasma gondii genomes. Nat. Commun. *7,* 10147.

1202 Luo, L., Bokil, N.J., Wall, A.A., Kapetanovic, R., Lansdaal, N.M., Marceline, F., Burgess,
1203 B.J., Tong, S.J., Guo, Z., Alexandrov, K.*, et al.* (2017). SCIMP is a transmembrane non-
1204 TIR TLR adaptor that promotes proinflammatory cytokine production from macrophages.
1205 Nat. Commun. *8,* 14133.

1206 McLeod, R., Boyer, K.M., Lee, D., Mui, E., Wroblewski, K., Karrison, T., Noble, A.G.,
1207 Withers, S., Swisher, C.N., Heydemann, P.T.*, et al.* (2012). Prematurity and severity are
1208 associated with Toxoplasma gondii alleles (NCCCTS, 1981-2009). Clin. Infect. Dis. *54,*
1209 1595-1605.

1210 McLeod, R., Skamene, E., Brown, C.R., Eisenhauer, P.B., and Mack, D.G. (1989).
1211 Genetic regulation of early survival and cyst number after peroral Toxoplasma gondii
1212 infection of A x B/B x A recombinant inbred and B10 congenic mice. J. Immunol. *143,*
1213 3031-3034.

1214 Mineo, J.R., McLeod, R., Mack, D., Smith, J., Khan, I.A., Ely, K.H., and Kasper, L.H.
1215 (1993). Antibodies to Toxoplasma gondii major surface protein (SAG-1, P30) inhibit
1216 infection of host cells and are produced in murine intestine after peroral infection. J.
1217 Immunol. *150,* 3951-3964.

1218 Nguyen, T.T., Klasener, K., Zurn, C., Castillo, P.A., Brust-Mascher, I., Imai, D.M.,
1219 Bevins, C.L., Reardon, C., Reth, M., and Baumgarth, N. (2017). The IgM receptor
1220 FcmuR limits tonic BCR signaling by regulating expression of the IgM BCR. Nat.
1221 Immunol. *18,* 321-333.

1222 Nussenzweig, R.S., Vanderberg, J., Most, H., and Orton, C. (1967). Protective immunity
1223 produced by the injection of x-irradiated sporozoites of plasmodium berghei. Nature *216,*
1224 160-162.

1225 Pape, K.A., Taylor, J.J., Maul, R.W., Gearhart, P.J., and Jenkins, M.K. (2011). Different
1226 B cell populations mediate early and late memory during an endogenous immune
1227 response. Science *331,* 1203-1207.

1228 Pedersen, G.K., Adori, M., Khoenkhoen, S., Dosenovic, P., Beutler, B., and Karlsson
1229 Hedestam, G.B. (2014). B-1a transitional cells are phenotypically distinct and are lacking
1230 in mice deficient in IkappaBNS. Proc. Natl. Acad. Sci. U. S. A. *111,* 4119.

1231 Pedersen, G.K., Adori, M., Stark, J.M., Khoenkhoen, S., Arnold, C., Beutler, B., and
1232 Karlsson Hedestam, G.B. (2016). Heterozygous Mutation in IkappaBNS Leads to
1233 Reduced Levels of Natural IgM Antibodies and Impaired Responses to T-Independent
1234 Type 2 Antigens. Front. Immunol. *7,* 65.

1235 Rowland, S.L., Leahy, K.F., Halverson, R., Torres, R.M., and Pelanda, R. (2010). BAFF
1236 receptor signaling aids the differentiation of immature B cells into transitional B cells
1237 following tonic BCR signaling. J. Immunol. *185,* 4570-4581.

1238 RTS, S Clinical Trials Partnership. (2015). Efficacy and safety of RTS,S/AS01 malaria
1239 vaccine with or without a booster dose in infants and children in Africa: final results of a
1240 phase 3, individually randomised, controlled trial. Lancet *386,* 31-45.

1241 Sacks, D.L. (2014). Vaccines against tropical parasitic diseases: a persisting answer to a
1242 persisting problem. Nat. Immunol. *15,* 403-405.

1243 Savage, H.P., Klasener, K., Smith, F.L., Luo, Z., Reth, M., and Baumgarth, N. (2019).
1244 TLR induces reorganization of the IgM-BCR complex regulating murine B-1 cell
1245 responses to infections. Elife *8,* 10.7554/eLife.46997.

1246 Sayles, P.C., Gibson, G.W., and Johnson, L.L. (2000). B cells are essential for
1247 vaccination-induced resistance to virulent Toxoplasma gondii. Infect. Immun. *68,* 1026-
1248 1033.

1249 Schuster, M., Annemann, M., Plaza-Sirvent, C., and Schmitz, I. (2013). Atypical IkappaB
1250 proteins - nuclear modulators of NF-kappaB signaling. Cell. Commun. Signal. *11,* 23-23.

1251 Schuster, M., Glauben, R., Plaza-Sirvent, C., Schreiber, L., Annemann, M., Floess, S.,
1252 Kuhl, A.A., Clayton, L.K., Sparwasser, T., Schulze-Osthoff, K.*, et al.* (2012).
1253 IkappaB(NS) protein mediates regulatory T cell development via induction of the Foxp3
1254 transcription factor. Immunity *37,* 998-1008.

1255 Smith, F.L., and Baumgarth, N. (2019). B-1 cell responses to infections. Curr. Opin.
1256 Immunol. *57,* 23-31.

1257 Splitt, S.D., Souza, S.P., Valentine, K.M., Castellanos, B.E., Curd, A.B., Hoyer, K.K., and
1258 Jensen, K.D.C. (2018). PD-L1, TIM-3, and CTLA-4 blockade fail to promote resistance to
1259 secondary infection with virulent strains of Toxoplasma gondii. Infect. Immun.

1260 Stumhofer, J.S., Silver, J.S., and Hunter, C.A. (2013). IL-21 is required for optimal
1261 antibody production and T cell responses during chronic Toxoplasma gondii infection.
1262 PLoS One *8,* e62889.

1263 Suzuki, K., Okuno, T., Yamamoto, M., Pasterkamp, R.J., Takegahara, N., Takamatsu,
1264 H., Kitao, T., Takagi, J., Rennert, P.D., Kolodkin, A.L., Kumanogoh, A., and Kikutani, H.
1265 (2007). Semaphorin 7A initiates T-cell-mediated inflammatory responses through
1266 alpha1beta1 integrin. Nature *446,* 680-684.

1267 Suzuki, Y., and Remington, J.S. (1990). The effect of anti-IFN-gamma antibody on the
1268 protective effect of Lyt-2+ immune T cells against toxoplasmosis in mice. J. Immunol.
1269 *144,* 1954-1956.

1270 Touma, M., Antonini, V., Kumar, M., Osborn, S.L., Bobenchik, A.M., Keskin, D.B.,
1271 Connolly, J.E., Grusby, M.J., Reinherz, E.L., and Clayton, L.K. (2007). Functional role for
1272 I kappa BNS in T cell cytokine regulation as revealed by targeted gene disruption. J.
1273 Immunol. *179,* 1681-1692.

1274 Touma, M., Keskin, D.B., Shiroki, F., Saito, I., Koyasu, S., Reinherz, E.L., and Clayton,
1275 L.K. (2011). Impaired B cell development and function in the absence of IkappaBNS. J.
1276 Immunol. *187,* 3942-3952.

1277 Waffarn, E.E., Hastey, C.J., Dixit, N., Soo Choi, Y., Cherry, S., Kalinke, U., Simon, S.I.,
1278 and Baumgarth, N. (2015). Infection-induced type I interferons activate CD11b on B-1
1279 cells for subsequent lymph node accumulation. Nat. Commun. *6,* 8991.

1280 Yang, Y., Ghosn, E.E., Cole, L.E., Obukhanych, T.V., Sadate-Ngatchou, P., Vogel, S.N.,
1281 Herzenberg, L.A., and Herzenberg, L.A. (2012). Antigen-specific antibody responses in
1282 B-1a and their relationship to natural immunity. Proc. Natl. Acad. Sci. U. S. A. *109,* 5382-
1283 5387.

1284 Yap, G.S., and Sher, A. (1999). Effector cells of both nonhemopoietic and hemopoietic
1285 origin are required for interferon (IFN)-gamma- and tumor necrosis factor (TNF)-alpha-

1286 dependent host resistance to the intracellular pathogen, Toxoplasma gondii. J. Exp.
1287 Med. *189,* 1083-1092.

1288 Zhao, K., Wang, Z., Hackert, T., Pitzer, C., and Zoller, M. (2018). Tspan8 and
1289 Tspan8/CD151 knockout mice unravel the contribution of tumor and host exosomes to
1290 tumor progression. J. Exp. Clin. Cancer Res. *37,* 312-6.

1291